R&D 5548-MS-01

(1)

"The Sol-Gel-Xerogel Transition etc."
Contract DAJA 45-89-0024, the US Army
Final Report - November 1993

D. Avnir
Department of Organic Chemistry
The Hebrew University of Jerusalem
Jerusalem 91904, Israel

Abstract. This contract supported the development of the technology of trapping of organic molecules and enzymes in porous sol-gel matrices. Our work led to the preparation and design of a wide range of novel optical materials. We summarize past achievements and recent progress made in the development of several classes of these materials, representing the diversity that the trapping approach allows: Chemical sensors, enzymatic sensors, electrooptical liquid crystal materials, luminescent materials and photochromic materials. Emphasis in this Report is given to our own results, and in addition, results from other laboratories, which are based on our developments and which are of high relevance to the topic of the Project (e.g., liquid crystal sol-gel displays), are summarized as well: we regard these other technological fruits a direct outcome of our sol-gel research.

1. Introduction

The five years that passed since the original Research Proposal was prepared (early 1989) have witnessed a tremendous, almost explosive, progress in the field of organically doped sol-gel glasses: Some 40 laboratories world-wide have been applying the new technology we developed of doping of ceramic sol-gel matrices with organic and bioorganic molecules, with applications ranging from optics to sensing to biotechnology and to catalysis. Since by and large all of these developments are due to our own work, we thought it suitable to report in the following pages not only on our own research, but to comment also on relevant achievements in other laboratories, whenever these achievements are a direct outcome of our sol-gel research (and in particular on sol-gel liquid crystal optics).

Sol-gel technology [1,2] triggered the birth [3-5] of this new class of materials with applications in two major domains: Optically active materials; and chemically active materials with good optical properties. Examples for the former include filters, luminescent materials, light guides, laser components, and a variety of materials for information processing and recording purposes [6]. Examples of the latter include a wide variety of sensors, bioactive sol-gel matrices in which enzymes are trapped, photoactive materials and catalysts [6].

2. Chemical sensing applications of doped sol-gel glasses

2.1. Introduction - Photometric Sensors

Photometric analyses are based on chemical interaction of photometric reagents with the analyte and detection of the emitted radiation (chemiluminescence) or analysis of chromophoric by-products by adsorption spectroscopy, fluorescence, phosphorescence or light scattering. A desirable photometric support is, therefore, a matrix that entraps the photometric reagents but leaves them exposed to exogenic analytes, with minimal chemical interaction or interference with the source and emitted light.

The properties of porous silica make it especially promising for photometric sensing because it combines the following desirable properties: a) rigidity, i.e. resistance to physical deformation and negligible swelling in liquids; b) chemical inertness which implies low interaction with the analyte and high photochemical, biodegradational and thermal stability; and c) excellent optical transparency in the visible and near UV regions. The missing link between the advantages of silica glass and their use in sensing technology is a method that allows immobilization of photometric reagents (which are mostly organic substances) in the solid support while maintaining its favorable properties without losing the reactivity and specificity of the embedded photometric reagents.

2.2. **Relevant characteristics of the sol-gel process.**

Before referring to the analysis of the characteristics of immobilization process in sol-gel matrices, the inherent pros and cons of the sol-gel process itself have to be considered. Sol-gel technology offers sensing industry the following advantages:

1. Control of *pore size distribution by simple* modification of the polymerization protocol. Monolithic supports that exhibit pore sizes which are smaller than the emitted and source wavelength reduce light scattering and increase sensing sensitivity. Exclusion phenomena can be exploited, by a proper choice of pore size distribution, to increase detection selectivity. Currently, the pore size distribution of sol-gel glasses is too flat, thus limiting size exclusion selectivity. However, Bein et al. [7] demonstrated that silica thin films doped with zeolite crystals (>1 μm, ZSM-5) benefit from the size exclusion selectivity of the encased zeolites.

2. Control of the surface area, void fraction and the geomettry of the supporting matrix. The ability to tailor desired configurations may benefit specific applications. For example, Grattan et al. [8] demonstrated that it is possible to mold doped sol-gel layer directly in a cavity formed by etching the very end of a

commercial optic fiber, thus attaining a configuration that has been traditionally expected only from polymer supports.

3. Freedom to choose appropriate supporting metal oxides, including titania, zirconia, silica and mixed oxides.

4. Control of the polarity of the glass e.g. by incorporating alkoxisilane compounds containing a desirable functional group [9] or by derivatization of preformed sol-gel pellets using the conventional protocols for silica derivatization [10]. Such techniques were used to reduce the quantity of silanol functional groups in sol-gel glass [11] and in order to improve the leaching characteristics of pH sensors [12].

Notable drawbacks of the sol-gel technology include:

1. Lack of large scale production know-how.

2. Hydrolysis of the SiO_2 network at high pH.

3. Fracture of monolithic glasses during gelation and drying or upon immersion in aqueous solution [13]. This can be partially circumvented by incorporation of drying control chemical additives, such as formamide and Triton-X [14] in the polymerization stage. However, formamide leaks off the glass in aqueous solutions causing fractures to appear after repeated dry-wet cycles. We have recently demonstrated [15] that doping of sol-gel glasses with a few percent of quaternary ammonium compounds (such as cetylpyridinium bromide and cetyltrimethyl ammonium bromide) prevents most of the gelation fractures and improves the leaching stability [16]. By introducing fracture prevention agents during the polymerization stage it is possible to avoid fracture even after many cycles of wetting and drying [15,17]. However, incorporation of fracture prevention agents narrows the window of optical transparency of the sensors and may limit some applications.

4. Ion exchange capacity of surface silanol groups: Surface silanol groups function as ion exchange centers, affect the pH and interfere with some aqueous photometric analyses (e.g. detection of heavy metals). The derivatization and copolymerization procedure that reduces hydrophobicity of the glass can also be used to reduce the ion exchange capacity.

2.3. Methods to immobilize reagents in solid supports.

Currently, impregnation, chemical derivatization and the newly introduced sol-gel doping are the possible technologies to encapsulate chemical reagents in porous supports. Similar methods are used to manufacture both inorganic supported sensors, such as alumina, titania and silica and polymer support sensors, such as styrene-divinyl benzene copolymer, PTFE, PMMA and other transparent organic polymers [18,19]. The same technologies are also used to manufacture chromatographic packings [20].

A. Impregnation and adsorption techniques: The organic reagents are physically adsorbed, chemisorbed or physically encased in porous supports (e.g. silica gel, alumina). Typical impregnation procedures are carried out by exposing the porous support to a concentrated solution of the reagent in organic solvent and discarding the solvent after equilibration, thus, after drying, obtaining a reagent coated support [21]. The technology is versatile; the same solvents, manufacturing apparatus and impregnation protocol can be used to encapsulate different reagents in a variety of organic and inorganic matrices. However, the adhesion of reagents to the support is rather weak, thus excluding *in-vivo* applications and limiting the practical operation and shelf-life of the sensors. Only when the leaching driving force is low (e.g. water exclusion by apolar matrices or gas analysis [22]) can such a device maintain long operation life. Otherwise, application of impregnation is restricted to disposable or renewable devices.

B. Chemical immobilization: Direct chemical bonding of organic reagents to silica supports gained much interest with the proliferation of chromato- graphic applications in the seventies and early eighties. For example, a siloxane bond (solid matrix≡Si-O-Si-C-reagent) is formed by a condensation reaction of reagent-chlorosilane precursor with surface silanol groups. Immobilization by chemical bonding has found many applications in chromatography [20], electrochemistry [23], and photometric detection [24] due to the high stability of chemical bonds. However, this type of encapsulation is highly specific so that reaction conditions and precursors have to be tailored for each case. This limits the application of chemical derivatization to expensive devices or to general purpose tools amenable to mass production such as chromatographic packing and capillary tubes.

C. Impregnation through molding - chemical doping. Traditionally, this method has been used to entrap organic compounds during the molding or polymerization of organic polymers. The method is exceptionally popular due to its high versatility and has found applications in the production of supporting membranes for diagnostics, separation purposes and organic and biochemical syntheses [25,26]. Until recently, the application of this technology was restricted almost exclusively to organic polymer supports, the only exception being the incorporation of inorganic compounds in inorganic matrices [10]. The advent of low temperature sol-gel synthesis of metal oxides opened the road to the development of similar inorganic/organic combinations.

Table 1 compares product characteristics of all three methods of encapsulation of organic reagents in silica supports. This comparison is based on general characteristics and, like in most general statements, a case by case inspection will, no doubt, reveal many exceptions to the rules. Generally, doped glasses exhibit properties which are intermediate between physical impregnation and chemical bonding. Doping technology is similar to impregnation techniques in its general application: the same procedure can be applied with little modification to encapsulate a

plethora of organic reagents [27]. As in impregnation technology, no derivatization of the chemical reagent is required prior to the encapsulation. Thus, reactivity and specificity of the dopant are generally maintained, except for effects of chemisorption and intraparticle microenvironment. Since the cavities produced by the chemical doping are not hermetically sealed, at least a part of the doped reagent is free to move between them. This limited mobility is of value when formation of a chromophoric group requires the participation of several ligands to form multiple ligand chelates. For example, iron(II) forms a three ligand orange-red chelate with o-phenanthroline (ferroine), but chemical bonding of o-phenanthroline to silica glass was reported to produce only a two ligand chelate [28], which obviously modifies the nature and specificity of the photometric product. o-Phenanthroline doped silica detectors produce exclusively the three ligand ferroine chelate, as can easily be verified by its UV/VIS absorption spectroscopy [29]. The observations of relative mobility are supported by the ESR (Electron Spin Resonance) studies of Ikoma et al. [30] demonstrating that polyamine copper(II) chelates entrapped in wet sol-gel alumina exhibit almost free tumbling motion. The mobility of reagents in the silica support also brings about better performance of the doped reagent and thus contributes to the increase in the practical capacity and detection range of silica sensors. However, the penalty for these advantages is paid by increased leaching of organic reagents from doped glasses. Free motion is not restricted to the ability to form multiple ligands but also means an ability to reach the solid liquid interphase and leak out. This is a considerable drawback since even a small leak of reagents from a sensor affects its long term performance and excludes *in vivo* medical applications. The long term stability of doped silica sensors is expected to be intermediate between impregnated and chemically immobilized sensors. However, it is clear that at this early stage it is premature to draw conclusions regarding long term stability and shelf life, although it is clearly high.

Table 1. Characteristics of immobilization procedures

Immobilization Process:	Impregnation	Covalent Bonding	Sol-Gel Doping
Generality	General	Specific	General
Properties of reagent	Maintained	Altered	Maintained
Intraparticle Mobility	High	Low	Intermediate
Leachibility	High	Low	Intermediate
Complexation Capacity	High	Low	High
Stability	Low	High	Intermediate
Shelf Life	Low	High	High
Manufacturing Cost	Low	High	Intermediate

2.4. Feasibility studies

The first reports of doped sol-gel sensors concentrated on qualitative feasibility studies using fluorimetric or colorimetric sensors.

Colorimetric devices: Zusman et al. [31] demonstrated qualitative colorimetric sensors for the detection of Fe(II) (o-phenanthroline), Ni(II) (dimethyl glyoxime), Cu(II) (α-benzoin oxime), SO_4^{2-} (sodium rhodizonate + barium fluoride) and several pH indicators. Nagomi and coworkers [32] noted that Cd-doped silica glasses prepared by the sol-gel technique change their color to yellow when exposed to H_2S due to the formation of CdS crystals. Zink and Dunn [33] reported that sol-gel glasses doped with iron(III) produce an intense blue color (Persian blue precipitate) when exposed to a solution containing hexacyanoferrate. Frye et al. [34] noted that organically modified glasses (Ormosils) derivatized by a diethylenetriamine compound (using $(CH_3O)_3Si(CH_2)_3NH(CH_2)_2NH(CH_2)_2NH_2$ asprecursor)chelatesCu^{2+} and can be used to sense atmospheric ammonia by formation of the intense blue color of copper amine. Useful environmental applications of doped SiO_2 sol-gel include sensors for detection of typical anions (NO_2^-, SO_4^{2-}), cations (Al^{3+}),heavymetals

[Co(II), Fe(II), Cd(II), Ni(II), Pb(II), Cu(II), Zn(II)], pH and redox potential indicators.

Fluorescence sensors: Following our finding that pyranine can be used as a sensitive fluorimetric probe for water consumption and release during the early stages of the SiO_2 sol-gel transition, Knobbe and coworkers [35] noted that the emission spectrum of pyranine doped silica glass is sensitive to the surrounding pH and that this phenomenon can be exploited to produce fluorimetric sol-gel sensors for pH. Reisfeld and coworkers [36,37] demonstrated that sol-gel silica (in thin film or monolithic rod configurations) doped with a pH sensitive dye (oxazine-170 perchlorate) may serve as a reversible colorimetric or fluorimetric sensor for airborne ammonia and acids.

Finally, Braun et al [38] demonstrated the possibility to entrap enzymes in sol-gel silica supports, thus opening the road for a variety of potential diagnostic applications. This application is detailed in Section 3.

2.5. Quantitative photometric applications

The field of chemical sensing using doped sol-gel is now evolving from a qualitative stage to quantitative prototypes, paying more attention to the chemometric characteristics of the device. At the time this chapter is written, no application has yet reached a stage of commercial exploitation or of performance evaluation by interlaboratory studies. However, some applications have reached quantitative stages where some characteristics can be drawn. In some cases the integration of sol-gel sensors into detection devices was successfully performed.

On-line fiber optic detectors: To date, on-line sensing by doped sol-gel glasses is confined to pH determination, most probably due to the size of the hydronium ion and its high mobility. Thus, it is relatively easy to prepare glasses in which bulky indicator molecules exhibit very low leachability while still being accessible to H_2O, H_3O^+, OH^- and other small molecules [39]. We

[39] and several other groups [40-42] examined the possibility to utilize a combination of sol-gel detectors with optic-fiber light conduction for detection of pH: Badini et al. [40] demonstrated fluorescence detection of pH using doped sol-gel silica films casted in a cavity formed by chemical etching of the end of a fiber optic. MacCraith et al. [41] used argon-ion laser source and sol-gel coated fiber-optic as a wave guide for evanescent wave excitation of fluorescein dye. We have recently constructed a pH sensor operated in an adsorption spectroscopy mode [39]. The detector is composed of a monolithic silica sensor doped with standard pH indicators, optical fibers for light conduction, a white light source and a spectrally sensitive detector. Using the ratio between the transmitted radiation at two (peak) wavelengths rather than measurement at a single wavelength improved stability and reduced drifts. Ding et al. [42] used fiber optic coated by a thin film of sol gel silica doped with commercial (colorimetric) pH indicators to measure pH changes in the range pH=3-9 by a single probe. The sensor exhibited high thermal stability and did not lose sensitivity even after heating to 200°C for two hours.

Cumulative Detectors: Dulebohn et al. [43] used spin coated titania glass thin film doped either with Eu^{+3} cryptate complex or with native Eu^{+3} ions to detect 4-*tert*-butylbenzoate and benzoate in aqueous solution. Detection is based on the increase in emission intensity of the lanthanide cryptates in the presence of Light Harvesting Centers (LHC) such as benzoate or tertbutylbenzoate ions. Dulebohn et al. demonstrate a linear operation range of such sensor in the range of 10-100 mM benzoate in aqueous solution. Despite the very thin layer (app. 0.6 μm) a typical response time is approximately 30 minutes, reflecting the low diffusion coefficients of the organic compounds in the porous silica.

Lev et al. [15] demonstrated quantitative monolithic detectors for the detection of iron, cobalt and cadmium. These three compounds were selected to represent three different classes of chelates: 1. Soluble covalently bonded iron-o-phenanthroline complex; 2. ion

pair complex of eosin Y with o-phenanthroline-cadmium chelate; and 3. insoluble salt of cobalt-1- nitroso-2-naphthol. In all cases "s" shape calibration curves depicting absorbance intensity versus analyte concentration were found. Exceedingly low detection limits (ca. 100 ppt, parts per trillion) were demonstrated due to the accumulation of the ions from the sample solution into the monolithic sensors [44]. This cumulative property was demonstrated by increased response sensitivity of sensors immersed in larger volumes of iron(II) samples.

Tube detectors: Tube detectors are vials containing glass pellets impregnated with colorimetric reagents [45]. When air is sampled through such a tube detector the analyte reacts with the reagent to form a colored section of the packed bed, the length of which depends on the concentration of the analyte in the sampled air. Due to the low adhesion of impregnated coatings, tube detectors suffer from relatively short shelf life (1-2 years) and are currently not suitable for aqueous analysis. We have recently demonstrated [46] that sol-gel detectors using sol-gel pellets doped with pH indicators can be used to determine airborne alkalinity and acidity. Such tube detectors may benefit from the increased stability of the sol-gel immobilization technology.

Tube detectors using packed beds of doped sol-gel glasses can also be used for the analysis of aqueous pollutants [47]. Capillarity or external driving force may be used to drive the solution through the detectors. This successful application is based on the fact that reagent leaching during the staining time is negligible. Interference studies of iron detectors (with o-phenanthroline SiO_2 glasses) revealed that the mode of interference was different from that of aqueous analysis [48]. Thus, in some cases, liquid phase interferences (e.g. nickel) were eliminated by displacement mechanism separating the bands of the interfering substance from the ferroine band. In other cases (e.g. zinc), when the interfering and the determined substances had similar affinity to the doped ligands significant interference was observed even when the interfering ion formed an uncolored complex with o-phenanthroline.

Repeatability studies using 24 different detectors revealed ca. 2-3% relative standard deviation of (0.2 mM and 10 mM) iron(II) determination. Bias and accuracy analysis revealed that irreproducibility in the preparation of the stock solution exceeded the bias level.

Another potential application of sol-gel tube detectors is for the analysis of water alkalinity [11]. Since alkalinity represents an integral measure of the buffer capacity of water, its determination is currently based on titration with strong acid. Using tube detectors containing sol-gel glasses doped with pH indicators (e.g. methyl-orange or bromocresol-purple), the sampled water titrates the glass surface silanol groups and the embedded indicators. Thus, the length of the stained section depends on the alkalinity of the solution and the sensitivity of the response depends on the sampled volume. Copolymerization, using larger ratio of methyltrimethoxysilane and tetramethoxysilane lowers the concentration of silanol groups in the glass and thus increases the sensitivity of the alkalinity detectors. Similar sol-gel glasses doped with pH indicators in their alkaline form can be used for the determination of water acidity.

3. Sol-Gel Immobilized Enzymes: Towards the Development of a New Class of Optical Sensors

3.1. Why Are There so Few Fiber-Optic Biosensors?

There exist a considerable number of clinical situations in which continuous *in situ* or on-line monitoring of solute concentrations in body fluids could be therapeutically advantageous. Among such analytes, whose importance is widely recognized are CO_2, O_2, H^+, K^+ and Ca^{2+} ions, glucose, lactate, creatinine and urea. The range of biological monitoring is likely to expand considerably in the future to include measurements of therapeutic concentrations of various drugs applied in controlled delivery systems.

The complex nature of body fluids imposes a tremendous degree of selectivity and sensitivity upon the interaction between the analyte and the sensor. One can safely assume that in the

predictable future no chemical or physical sensor would be able to compete in selectivity or sensitivity with biological recognition systems provided by protein molecules. Indeed, enzymes, receptors and antibodies have been applied to detection and measurement of many, if not most, medically important substances.

Recent development of fiber optic techniques and their application in the sensor technology stressed the advantages of optical devices over electrochemical sensors in solving the problems of continuous monitoring (Table 2).

Table 2. Advantages of Optical Sensors

1. No need for a reference electrode;
2. The signal is not influenced by electrical "noise";
3. The sensor can be manufactured as a miniature disposable element mechanically connected to the optical fiber;
4. Simple factory or one-point calibration;
5. Simultaneous measurement of several analytes by co-immobilized sensor reagents at different wavelengths;
6. Optical control of the baseline stability.

Electrochemical devices are inherently limited to reactions involving ion movements or electron transfer, while a modification of reactant optical properties is almost inherent in every chemical (biochemical) reaction. The current practice of biochemistry is, indeed, considerably richer in optical than in electrochemical detection techniques. Paradoxically, most, if not all, existing continuous enzyme sensors are enzyme electrodes. The reason for this discrepancy can be found in general limitations of optical sensor devices (Table 3).

Table 3. Limitations of Optical Sensors

1. Limited dynamic range;
2. Signal amplitude depends upon the amount of reagent in the optical pathway;
3. Photobleaching or photodegradation of the sensor reagent.

Limited dynamic range is a general shortcoming of continuous enzyme sensors both optical and electrical; it is determined by the saturative nature of the enzyme response. The complete concentration range of an enzymatic reaction between the basal and the maximal responses is exhausted within one order of magnitude. The main obstacle to widespread use of optical sensors is, however, in the very nature of signal generation. The signal amplitude is directly proportional to the amount of a chromophore in the optical pathway. The usual media for enzyme immobilization are not suitable for spectroscopic measurements, since they have very short optical pathways. Porous matrices with large surface areas, suitable for containing large amounts of enzymes, are opaque; the light is dispersed at the solid-liquid interface. Thus, optical sensors may be engineered either by coating the surface of an optical fiber with the immobilized enzyme, or by including non-immobilized water-soluble systems contained in porous membranes and attached to the fiber [49]. Both solutions are less than satisfactory. Surface coating limits the amount of the sensor reagent to less than a monolayer. Water-soluble systems are unstable, have to be contained within a semipermeable membrane, and are difficult to manufacture.

3.2. The Sol-Gel Option

The search for stable transparent matrices suitable for optical biosensors attracted our attention to sol-gel glass materials. As mentioned above, they are mechanically and chemically stable, highly porous hydrophilic materials, which do not swell appreciably upon hydration, pH or ionic strength changes. This material may be easily manipulated to produce any desired geometry including thin films and optical fibers.

We have demonstrated recently [38,50-53] that proteins could be entrapped within the matrix of a forming sol-gel, while retaining high enzymatic activity. Upon drying, these sol-gels form transparent xerogels. Dry xerogels preserved the biological activity of immobilized enzymes, which could be recovered after rehydration [49]. A large number of enzymes has been successfully immobilized using different variations of a simple procedure in which an enzyme solution is mixed with partially hydrolyzed sol-gel precursors (tetra-alkoxy and trialkoxy alkyl-silanes) [50-53].

Good optical properties depend upon the unique microstructure of sol-gel silicas [52]. Scanning electron microscopy (SEM) of protein-containing xerogels prepared from tetramethoxy-ortho-silicate (TMOS) demonstrated mesoporous microstructure of fused silicate globules roughly 0.1 μm in diameter (Fig. 1). N_2-BET surface area [52,53] of such gels was 500-700 m^2/g regardless of protein content (3-30 mg/g). Lower initial pH resulted in larger BET surface areas (650-700 m^2/g at pH 2-5). With further increase in pH, surface areas gradually decreased, measuring 500-550 m^2/g at pH 12. A concomitant increase in pore volume was observed (0.3-0.4 ml/g at pH 2 versus 0.7-0.9 ml/g at pH 12). The volume of pores depended upon protein load. Thus, pore volumes decreased from 0.6 ml/g at 3 mg trypsin/g xerogel to 0.2 ml/g at 30 mg/g. All xerogels had a very narrow pore size distribution. The average pore diameter was 3-4 nm at pH 2, and increased to 7-10 nm at pH 7 with slight variation above this pH. These small and uniform pores do not generate significant light dispersion.

Most protein-containing xerogels could be obtained as monolith transparent glasses of a considerble mechanical strength [52,53]. In our hands most of the proteins did not aggregate during xerogel preparations even at concentrations up to 30 mg/g glass. Some proteins, such as e.g. bovine serum albumine (BSA) or alkaline phosphatase formed cloudy protein aggregates [49,52,53]. The aggregation seems to occur when a protein molecule was not adsorbed on the gel-phase of the forming sol-gel, it was, rather,

excluded into the free water phase. To a considerable extent the partition of a specific protein could be modified by the initial pH of the sol, addition of charged monomers etc. Since adsorption of proteins to most surfaces, including silica, increases with the increase of protein molecule hydrophobicity, [54,55], an efficient sol-gel immobilization of an enzyme, both in terms of its activity and the transparency of the gel, is expected at pH values close to its isoelectric point (pI) [53].

Enzyme entrapment in a gel matrix is a convenient and generally applicable immobiolization technique, which does not require tedious chemical derivatization procedures for the protein coupling. Unlike currently used matrix materials, enzyme-containing xerogels possess a very uniform array of communicating pores, thus, the loss of the enzyme by leakage through a nonuniform net of polymer molecules (the most common drawback of entrapment methods) is prevented. Enzymes immobilized in sol-gel xerogels do not leak even at harsh washing conditions [38,49-53].

The kinetics of sol-gel immobilized enzymes closely resemble that of the water soluble counterparts [50-52]. Variations of substrate concentration resulted in hyperbolic dose-response curves consistent with Michaelis-Menten kinetics. Thus, e.g. dose-response curves of trypsin-containing gels could be fitted within the limits of the experimental error to Michaelian forms. The parameters resulting from such fitting were: the K'_m = 0.80±0.06 mM, as that of the free trypsin, and the V'_{max} = 2.00±0.04 U/mg corresponding to 47% of the enzyme activity used in the preparation of the gel.

Enzymes entrapped in hydrogels usually do not interact with the matrix, and, thus, are able to diffuse. The ability of glass entrapped trypsin molecules to diffuse within the glass was tested by measuring the extent of its autodigestion. The free or loosely immobilized trypsin can completely degrade itself at a neutral or slightly basic pH. Bioactive sol-gel glasses obtained by a surface adsorption of trypsin to a readymade xerogel were also completley

inactivated either by autodigestion at 25°C overnight in a buffered solution (pH 7.5) or by a prolonged washing. In contrast, the sol-gel entrapped trypsin [52] retained full activity when incubated or washed at pH 7.5 at ambient temerture overnight, or even for several months(!). The existence of diffusional limitations indicated strong interaction between the silicate matrix and the protein molecules. It seems that during the polymerization there occurs an imprinting of the protein surface in the matrix resulting in tight binding [50-53]. As a consequence, considerable stabilization of the enzyme occurs. Thus, sol-gel immobilized alkaline phosphatase was more stable at 70°C than its soluble form [49]. An even more dramatic protective effect was observed in sol-gel immobilized preparations of acid phosphatase [50,52], which is considerably less heat-stable than its alkaline counterpart. Upon heating to 70°C, the soluble acid phosphatase quickly lost its activity (half-life time of less than 0.1 min). The immobilized acid phosphatase was more stable by two orders of magnitude.

Table 4. *Advantages of Sol-Gel Immobilized Biological Systems for Optical Monitoring Devices*

Transparency of the matrix;
High concentration of the sensor material;
Lack of protein leaching;
Considerable stabilization of the immobilized enzyme;
Shelf-life of at least a year at ambient temperature;
Simplicity of preparation;
Biocompatibility.

Sol-gel methods allow us to produce a unique sensor material containing homogeneously dispersed enzyme molecules forming a stable "solid solution" in a transparent medium. It has been shown that similar sol-gel materials are biocompatible [56]. Our attempts to utilize the advantages (Table 4) of sol-gel methods in the design of optical enzymic sensors has began with glucose assay devices.

3.3. Glucose sensors

Continuous monitoring or bedside estimation of blood glucose concentrations can greatly aid intensive care patients. Various non-enzymatic and enzyme electrode sensors have been designed to monitor glucose. Most of these sensors are based on covalently immobilized glucose oxidase. Electrode fouling, need for frequent baseline calibrations and other problems hinder their application.

In order to circumvent the problems of long-term biocompatibility, we have not selected a model of the *in vivo* sensor for, e.g., artificial pancreas, but a simpler sensor satisfying the requirements for the application in open heart surgery, or for blood monitoring during childbirth by a diabetic mother (Table 5). In any event, our goal was to test the feasibility of a sol-gel approach for such applications.

Table 5. Main Requirements for a Continuous On-Line Blood Glucose Monitor During Surgery

High specificity for gluocse;
Linearity of response from 1 to 15 mM glucose;
Response time less than 10 min;
Response independent of hydrodynamics and oxygen;
Variation in blood;
Lifetime of at least 24 h at 37°C in blood;
Shelf-life of at least a year at ambient temperature;
Biocompatibility (does not induce blood clotting);
Calibration (factory);
Construction (amenable to mass production).

The simple construction and the low cost of sol-gel immobilized enzyme sensors, allowed us to construct an irreversible, disposable sensor model based upon glucose oxidase and peroxidase chromagenic assay. The enzymes were dissolved in water, and then gently shaken with TMOS containing 0.5% polydimethylsiloxane. The resulting gel was allowed to dry at ambient temperature for 2 weeks. The transparent glassy xerogel was impregnated with a

chromagenic mixture [57] solution contining 3.3mM 3-(dimethyl-amino) benzoic acid (DMAB) and 2mM 3-methyl-benzothiazolinone hydrazone hydrochloride (MBTH) in 0.1 M phosphate buffer at pH 6.5. The xerogel was then air-dried.

Glucose oxidase and peroxidase catalyze the following reactions:

(a) *Glucose oxidase:* Glucose + O_2 = Gluconolactone + H_2O_2

(b) *Peroxidase:* Donor + H_2O_2 = Oxidized Donor + H_2O

MTBH was used as the electron donor in reaction (b), and the oxidized donor reacted with DMAB forming one mole of indamine dye per mole glucose [53]. The formation of dye in the glassy xerogel in the presence of glucose (Fig. 2) was recorded with a densitometer filtered at 595 nm. Kinentics of dye formation at various glucose concentrations demonstrate that the device was glucose-sensitive in the range between 0 and 100 mM.

A more useful sensor, devoid of the necessity to prevent the slow but existing loss of trapped dyes to the medium was based upon the difference of spectral properties between the reduced and the oxidized flavin prosthetic group in the enzyme glucose oxidase. Xerogel blocks (5x10 mm) prepared with glucose oxidase alone (10-15 mg/ml of the gelation mixture) have promptly (within a few minutes) changed their colour from the bright orange color of the oxidized flavin to the colorless reduced form in the presence of glucose. Removal of glucose resulted in the restoration of the color.

These are the first attempts to demonstrate the feasibility of sol-gel techniques in the building of optical enzyme sensors. The flavin prosthetic group is present in a variety of enzymes suitable for numerous tests, such as amino acids, sugars, various drugs, etc. Another promising group is hem proteins. Thus, a CO_2/O_2 sensor may exploit the differences in spectra of myoglobin [58] or hemoglobin (although in our hands, the glasses prepared according to the procedure described in this reference, cracked into small grains upon immersion in water, rendering it unsuitable for wet-sensing purposes). The sensors may be based not only on differences in absorption spectra, but also on luminescence or

fluorescence of various enzyme-substrate, enzyme-inhibitor or enzyme-antibody complexes, as well. The wealth of chromophores present in enzymes, or added to them by various techniques makes it possible to produce an enzymatic sol-gel sensor for almost any purpose.

The above two Sections demonstrated the use of chemically active doped sol-gel matrices with applications based on their optical properties. The next two Sections describe progress in optics application of organically doped glasses within which photophysical and electrooptical processes take place.

4. Sol-gel gel-glasses for electrooptics: the trapping of liquid crystals.

4.1. Gel-glass Dispersed Liquid crystal (GDLC)

Efforts are currently directed towards the development of electro-optical devices which have the required electrooprical properties and are easy to prepare as electrooptical devices. Electrooptical effects combined with certain processing steps can provide the basis for a wide variety of information processing and non-linear optical devices such as optical switches, displays or light modulators. Liquid crystals (LC) have gained a recognized role in physical science and in several electronic-related technologies. The present applications of LC are basically in the preparation of commercial electronic displays as well as low-voltage, easily driven electrooptical devices. At present, a major obstacle in the development of electrooptical devices is the lack of suitable materials which have both the required electrooptical properties and can also be made into usable forms such as thin films and bulk pieces.

The modified sol-gel process is well suited to provide a molecular oriented surface for the preparation of gel-glass dispersed liquid crystals in thin films. In general, the sol-gel process was used to avoid undesirable dye aggregation [3] usually observed in aqueous solutions. Levy, Serna and Oton [59,60] showed the

feasibility of trapping a "bunch" of molecules (droplets), in a thin film. In order to change the trapping technique and to modify the material properties these authors used a polymerizing organoalkoxysilane (e.g. CH_3CH_2-Si$(OCH_2CH_3)_3$). Therefore, their main concern was to ascertain whether the sample manufcturing keeps the LC structure. An important factor to avoid textural inhomogeneities in nematic microdroplets is the production of an orienting surface, i.e., using Si-CH_2CH_3 groups on the pore cage [59]. It may provide a lamellar structure for the LC molecules at the surface, an action that could be called a "molecular hair combing" that is sufficient to obtain molecular orientation and microliquid crystalline phases. In addition, Si-CH_2CH_3 groups provides flexibility to the matrix needed for deformations and reorganization of the microdroplets at the time that an electric field is applied to the doped thin film. The trapping process does not alter the electrooptical and thermal response of the LC. The trapping technique provides a convenient method for protection of liquid crystals from physical damage and extend the range of applications through increased flexibility in handling of the material.

The feasibility of the technique was demonstrated [59] and different combinations of liquid crystals (LCs) and substrates were studied [61]. A great deal of work was carried out to identify the experimental conditions that may influence the optical response of the materials. Either single monomers or mixtures of two monomers were employed to prepare GDLCs with different electrooptical responses [61]. In the second case, one of the monomerrs has four functionally reactive-site leaving groups, whereas the other has only three. Several monomers and mixtures at diffeerent reaction conditions were investigated [61], in order to vary the pore size and surface properties of the silica cages. GDLCs were prepared with these matrices using different LCs. The following LCs were tried: K15, E7, MBBA, Phase 5 (all nematics); The cholesteric cholesteryl linoleate (ChL), and the ferroelectric smectic C mixture ZLI-3775. All of them but ChL and MBBA (which probably hydrolized) have yielded droplets of

different sizes in several gel-glasses used in the early stages of the work; therefore ChL and MBBA were rejected for the moment, and subsequent experiments were performed on K15, E7, Phase 5, and ZLI-3775.

Several batches of GDLCs with different microdroplet sizes were prepared and the most promising GDLCs were selected according to their electrooptical performance [61]. Phenyl silicon and methyl silicon substrates were employed as orienting surfaces for trapped microdroplets of LC. GDLCs were obtained in most of the matrices and LCs tested. Droplets ranging from 2 to 200 μm were observed by optical polarized microscopy. Droplets below 1 μm must be present in some cases, as demonstrated by the switching behavior of several samples. Except for a few irregular droplets formed near the sample surface in some cases, all of the droplets were almost perfectly spherical (Fig. 3). In addition, a few samples show full coloured patterns with no visible droplets although some of them exhibit switching like usual samples.

Switching of the GDLC samples was observed by applying an AC voltage over threshold (i.e. high enough to switch the sample) to the conductive plates. The switching voltage was determined by measuring the light transmitted through the GDLC cell under AC fields. The voltage needed for switching was produced using a pulsed high frequency sinusoidal wave generator. The generator employs a 20 KHz sinusoidal carrier amplitude-modulated by a 0.5 Hz square wave signal. The carrier peak voltage can be varied from 0 to 120 V. When no voltage is applied, LC microdroplets scattered visible light, and the sample is white opaque or milky. The voltage reorients the LC director and the LC ordinary refractive index becomes the only one "seen" by the incoming light, thus reducing the index difference between LC and substrate. This reduces the scattering and the sample becomes more transparent. No polarizers are needed to produce the effect. If a completely transparent state is desired (i.e. Fresnel limited transmission), the substrate refractive index may be modified to match the ordinary index of the LC. Even in low LC concentration unmatched

GDLCs switching was observed with the naked eye. Therefore complete transparency is not achieved for the moment (e.g. T_{on} about 10-20%), and the contrast is poor (about 2-5:1). The actual contrast ratios obtained in these samples are very low, since no attempt was made to match the refractive index of the substrate (≈1.43) with the ordinary index of the liquid crystal. In other words, no Fresnel-limited transmission is achieved. Moreover the LC concentration (hence the scattering) is quite low; therefore the opaque state is not white but translucent, allowing a substantial fraction of light to get through the sample.

To characterize the orientation and shape of the microdroplets, the samples were switched in a microscope between crossed polarizers. Radial orientation [62] corresponding to a homeotropic surface condition was obtained in all cases, as shown by a characteristic "Maltese cross" pattern in the droplets. Single domain droplets were obtained in all cases but largest sizes (40 μm to 50 μm) consisting of multidomains were seldom detected. The droplets are spherical, their diameter varying ±20% within each sample. Droplets from 2 μm to 50 μm were obtained by controlling reaction conditions. Large variations in reaction times, thresholds and droplet sizes were found. It must be noted that the chemical composition of the pore walls is different in every case; we believe that most of the observed variations in GDLC formation and behavior may be attributed to this (see section 4.2).

The physical and optical properties of nematic microphases in GDLCs exhibit marked changes with temperature. Phase transitions, e.g. from nematic to isotropic phases, were marked by a sudden change in anisotropy and optical character. Micronematic phases are stable at room temperature, Fig. 3, and their structure is maintained. It was suggested that order arises as a consequence of the chemical affinity between the apolar character of the pore surface and the lipophilic groups of the LC.

Reorientation of the GDLCs was achieved with electrical and optical fields [59,61]. An Ar^+ laser focused onto the sample

produces several diffraction patterns which were previously described in planar and cylindrical LC samples [59]. This feature is observed in positive and negative nematic LCs, as expected. Reorientation of negative LCs applying voltage is observed by evolution of polarization textures in the microscope. No reorientation was detected in the ferroelectric LC (with either AC or DC pulses); this fact is presently under study. It is possible that some of the ZLI-3775 mixture components were separated or decomposed during the sol-gel process. Positive nematic LCs show switching to the naked eye. Switching times from several milliseconds to hundreds of milliseconds have been found [63]. Obviously, much work has to be done to characterize and optimize GDLCs in order to produce practical devices.

4.2. Parameters affecting the GDLC dynamic response

Substrate and liquid crystal: A different electrooptical behavior was found when varying the non-reacting organic group (e.g. methyl or phenyl) of the polymerizing organoacethoxy (or alkoxy) silane [63]. Phenyl samples (Fig. 4) show a much lower threshold voltage ≈10 V_p) than methyl samples (≈25 V_p). Once the threshold is surpassed, phenyl samples rapidly reach a constant rise time whereas methyl samples show a steady decrease over a ≈30 V_p range. The same behavior is found if normalized contrast ratios are plotted vs. applied voltage, Fig. 4.

LC concentration: A comparison of rise times for different LC concentrations in the same methyl substrate (two droplet size ranges were used) [63] shows (Fig. 5) that the rise time varies with the LC concentration, but negligible changes were detected with droplet size. When the applied voltage is increased, rise time reaches a constant value for every LC concentration. The lower the LC concentration, the lower the applied voltage needed for "saturation". On the other hand, fall (relaxation) time does not depend on the LC concentration.

Droplet size: The relation between relaxation time and droplet size for a methyl substrate was tested by comparing two different

pore sizes having two LC concentrations for each case. The relaxation time is fairly constant for the whole range of switching voltages and does not depend on the LC concentration; however a clear dependence on pore size was observed [63].

4.3. GDLC dynamic response

The parameters affecting the GDLC dynamic response [62-64] are linked to the substrate and LC mixture, to the LC concentration and to the droplet size. The results in Fig. 4 can be explained assuming weaker anchoring forces in the inner surfaces of phenyl pores than in methyl pores. This is confirmed by the longer relaxation time (t_{off}) of phenyl samples. The lower threshold for phenyl substrates was also found in that case. However, the samples showed faster switching times, as did alkyl homologous series. In any case, the conclusion of this comparison between phenyl and methyl substrates is that phenyl substrates are superior for optical shutters with either liquid crystal, whereas methyl substrates are better for applications requiring smooth variations of transmission with voltage, such as analog grey scales or variable birefringence devices.

The influence of different LC concentrations on rise time in methyl substrates was also studied. Fast rise times were found for low LC concentrations in methyl and phenyl series Fig. 5. This behavior may be related to the effective electric field that reorients the microdroplets in every case. The dielectric substrate has a fairly constant permitivity, but the presence of LC microdroplets induces inhomogeneities within the material. In other words, the electric field affecting a single droplet is shielded by the presence (and concentration) of other adjacent droplets (a higher voltage is needed to reach a steady rise time for higher concentrations).

Droplet size, as expected, affects the overall rise time values of a sample batch, but does not change with the applied voltage, which depends mainly on the LC concentration. However, the fall time is only dependent on LC relaxation mechanism, which

ultimately depends on surface anchoring forces. It seems obvious, therefore, that a larger pore size must increase the relaxation time. This effect is easily observed in sandwich cells of pure liquid crystal (i.e., without substrate), where relaxation times largely depend on cell thickness. A thicker cell (or a larger pore) means that the wall is farther, and a larger amount of material must be reoriented by a proportionally smaller surface (the ratio surface/volume decreases).

4.4. GDLC devices

The possibility of using GDLCs as electrically-controlled birefringence (ECB) devices was also analyzed. In this case, a continuously varying phase delay depending on the applied voltage must be demonstrated.

Preliminary results using GDLC materials open the possibility of manipulating light signals in photonic systems. Two kinds of devices could be derived from such materials: optical shutters and polarization controllers. The GDLC films presented above can be used as optical shutters simply matching the matrix refractive index with the ordinary index of the LC.

An alternative device can be obtained applying transverse electric fields to GDLC bulks. In this case, a variable birefringence is obtained (electrically controlled birefringence, ECB), the light output being controlled by suitable oriented polarizers. These devices must show a range of LC reorientations for different applied voltages, as found in methyl-based GDLCs. Some preliminary experiments on GDLC-films having methyl and phenyl groups on their inner pore surfaces have been performed. The birefringence of the ECB-GDLC is determined by the ordinary and extraordinary refractive indices (n_o and n_e) of the LC. At the off-state, light depolarization results from LC orientation in the microdroplets, controlled by anchoring forces and droplet shape. At the on-state, the electrically controlled LC reorientation in the microdroplets modifies the average refractive index. The sample becomes more birefringent, and the output light can be controlled with the

polarizers. Typically, the transmission axis of the first polarizer is oriented along the electrical field, and the second is crossed. In this case, a variable decrease of transmitted light (ideally down to complete extinction) is observed for different applied voltages. In a practical device, the substrate refractive index should have an intermediate value between n_o and n_e to reduce the scattering. The characterization and optimization of ECB-GDLCs are currently under study.

5. Organically doped sol-gel glasses for luminescent and photochromic optics.

5.1 Fluorescent and laser sol-gel glasses

Organic dye lasers have been found to play an important role in a variety of applications in optical systems, spectroscopy and lasers. Special attention has been given to solid matrices such as polymeric blocks and polymeric thin films in which the dye is homogeneously distributed. The disadvantages of these organic heterogeneous environments compared to the inorganic sol-gel matrix have been described in detail elsehwere [5]. For instance, the gel-glass formed in the sol-gel process is transparent deep into the UV (Fig. 6) in comparison to the commonly used dye carrier poly(methylmethacrylate) (PMMA) which filters light <330 nm. Rhodamine 6G (R6G) has been one of the most frequently used organic probes in these studies, due to its high fluorescence quantum yield and good lasing properties. Fluorescent dyes were both the first organic molecules which were incorporated in sol-gel glasses [3-5] and the most numerous as a class. Examples, in addition to R6G [5,65-68], include naphthazin [65], acridines [65], coumarines [65,66], rhodamine B [65,67,69-71] ruthenium complexes [67,72,73], fluorescein [67,74,75], crystal violet [66,67], malachite green [67], oxazines [37,66,67], 4-methylembelliferone [69], nile-blue [66], porphyrines [66], resorufin [66], cresyl-violet [66] and phthalocyanine [66]. Most of these were trapped in SiO_2 and Al_2O_3 matrices. Many of these glass preparations were used also for studying the properties of the glass cage [5,38,50,70,74,76-83], for photochemical hole

matrices [39,40,42], for obtaining laser emission [88-96], for studying non-linear optical effects [97-104], for the development of thin-film light-guides [67] and for the preparation of luminescent solar concentrators [105].

Although obtaining laser blocks was the very reason for our choice of rhodamine 6G as the first trapped organic molecule [5], it was not until 1988 that this concept was successfully demonstrated simulatneously by research groups in Japan [88,89] and in the USA [90]. One of the key problems in the investigation and application of organic laser dyes is the matrix which hosts the dye. The nature of the hosting matrix affects all characteristics of the dye, e.g., it causes spectral shifts of both absorption and emission spectra, it affects photostability and alters the distribution between processes that the excited state undergoes, such as intersystem crossing, collisional energy loss, and consequently also the fluorescence lifetime. The dimerization and aggregation processes of laser dyes have a strong effect on spectral and lasing properties. The sol-gel method overcomes this difficulty [5,67]. At $1x10^{-4}$M in water, R6G does not lase due to dimerization. When R6G is trapped in silica sol-gel gel-glasses, it does not aggregate much behind the limit of $1x10^{-4}$ (moles of dye per liter of glass) (e.g., Fig. 6). The fact that no dimers are observed may serve as an indication to the size of the cage: roughly that of a single molecule, i.e., 10A; under this restricted cage conditions, the molecule excited-state stabilization takes place by interactions with the surrounding cage. Otherwise, sufficient water would be trapped to form dimers at the high concentration employed. Kobayashi et al. [88] were able to reach dye concentrations as high as 10^{-2}M in alumina sol-gel without aggregation. Irradiation of the doped film with a nitrogen-laser produced laser emission with a beam divergence of 0.1 rad. It was found that the width of the dye laser emission was 10 nm, which is typical of dye lasers. The calculated conversion efficiency was 2.1% and it was found that the power decreases linearly with the number of shots, which is indicative of a single-photon process.

Later it was found [89] that increasing the concentration of the dye increased the pumping efficiency. This dependence indicates that the doped films operate as compact dye-laser films.

Lasing activity from sulforhodamine-640-doped silica sol-gel was recently reported by Salin et al. [92]. The doped glass was pumped with a frequency-doubled radiation from a Q-switched Nd:Yag laser, and a 20% conversion efficiency was obtained. The important aspect of that report is the 40 nm tunability of that material.

Recently, Canva et al. [96] reported a new sol-gel preparation technique: impregnation with a sol. The impregnation technique was found to enhance the mechanical properties of the material and greatly improves all the sample characteristics used in a laser cavity.

An important observation made in these studies has been the increase in thermal and photostability of the trapped dye. Trapping the dye molecules, their decomposition products and other impurities, de-aggregation, and reduction of both vibrational and rotational modes of energy dissipation, all contributed to the enhanced stability. This is of major practical consequence, for instance for blocks of dye lasers. Nakazumi et al. [107] showed that photostability of sol-gel coating gel films depends on organic dyes and, in some cases, on the matrix of the gel. They showed that photofading of methylene blue in thin films prepared from methyltriethoxy-silane is faster than in films prepared from tetraethoxysilane. Fujii et al. [70,74,76] have shown that the thermal stability of rhodamine B is enhanced in silica gel compared to ethanol solutions.

Efforts have also been devoted to enhance the photophysical properties of the trapped molecules by host matrix improvements. Pope et al. [69,108] and Capozzi et al. [97] prepared a new class of transparent silica gel-PMMA composites improving physical, mechanical and optical properties by increasing the deree of chemical coupling which exists between the silica gel and PMMA

phases. This led to a different approach in which laser-dyes and optically nonlinear dyes were not trapped by the sol-gel method, but adsorbed on the pores of the glass via an organic polymer solution. This approach, which is outside the scope of the present review, is described in reference 106.

The ability to trap photoactive organic molecules in the form of thin sol-gel films is shown in Fig. 7, in which the emission spectra of a variety of dyes belonging to various families are shown. Similar results were obtained for mixed titania-silica sol-gel thin films. As in the case of blocks, aggregation and leachability tests proved that the dyes are trapped in closed cages. The photostabilization of the trapped dyes, observed in the monolithic glasses, is also observed in the thin films.

5.2. Phosphorescent gel-glasses

Whereas in Section 5.1 we dealt mainly with emission from the singlet, i.e. fluorescence, here we briefly describe some interesting results concerning the emission from the triplet, i.e., phosphorescence. Phosphorescence is differentiated from fluorescence by the long-lived emission of light after extinction of the excitation source. The sensitivity of phosphorescence spectroscopy is comparable to that of fluorescence spectroscopy and complements the latter technique. The reluctance to use phosphorescence spectroscopy probably arises from the practical aspect of measuring the signal, since cryogenic temperatures, using liquid nitrogen at 77 K, are normally required. Recent developments in room temperature phosphoresence (RTP) have given rise to practical and fundamental advances which should help stimulate interest in phosphorimetry.

One of our main findings has been that trapping a wide variety of organic molecules in sol-gel gel-glasses, enables one to observe RTP from the trapped molecules [109,110]. This was demonstrated on the following molecules: phenanthrene, naphthalene, quinine, 4-biphenyl carboxylic acid (4-BPCA), 1-naphthoic acid, eosin-Y, and pyrene. The RTP characteristics of these organic molecules

trapped in silica gel-glasses are observable only under special conditions of reaction, and were detailed in reference 110. It was observed that most dyes emitted either phosphorescence or both delayed fluorescence and phosphorescence when the optimum conditions for gelation were established [110]. For example, under neutral conditions of gelation phenanthrene, naphthalene and quinine show good RTP signals. Basic conditions of gelation are required to observe phosphorescence emission for 4-BPCA, 1-naphthoic acid and eosin-Y, and the presence of a heavy atom perturber is necessary for the observation of the phosphorescence for pyrene.

The gel-glass itself is not fluorescent [5] or phosphorescent [110] and the trapped molecules are only slightly affected by external conditions like moisture and oxygen. A detailed study on the luminescence properties of 4-BPCA and 4-BPCA/NaBr molecules (Fig. 8) showed that phosphorescence intensity from the molecules trapped in the gel matrix are highly sensitive to environmental (cage) effects. The changes in the luminescence properties of this trapped molecule were studied as a function of several parameters that are responsible for the structural properties of the isolating matrix, such as variation of catalytic conditions of gelation, the addition of heavy atom perturbers to the starting mixture of the components of the gelation and heat treatment of the wet gel. When a NaOH solution was employed (instead of water) for the polymerization and trapping of 4-BPCA, the results showed that a 0.5 M NaOH (Fig. 9b) concentration provides the best conditions for the observation of phosphorescence, which was attributed to the anion of 4-BPCA. Concentrations higher than 0.5 M NaOH (Fig. 9c), provide strong delayed fluorescence and weak phosphorescence intensities. These originate from a mixture of the anion and non-dissociated states of 4-BPCA. Lowest NaOH concentrations and neutral conditions of reaction provide only delayed fluorescence (Fig. 9a). The addition of a heavy atom perturber to the initial solution results in an increase of phosphorescence intensity (Fig. 8). In some cases, RTP can be obtained from wet samples so that a drying process is not

essential. Drying, however, always enhances the phosphorescence intensity and lengthens the triplet lifetime by three orders of magnitude [110].

The spectroscopic changes were explained in terms of both solvent evaporation and increase in matrix density and cage rigidity [110]. In some cases, these changes eliminate most of the non-radiative processes by collisional deactivation of the triplet state of the molecule in the case of RTP. Recent studies on the photoisomerization of azobenzene in sol-gel glass films by Ueda et al. [111] have suggested that the sol-gel matrix is more rigid than a PMMA matrix and that the rigidity of the sol-gel glass is dependent on the starting solution water content. Molecular isolation in gel-glasses is very efficient: the resulting phosphorescence is stable for a long period of time (at least one year).

5.3. Photochromic gel-glasses

Photochromism is the phenomenon in which absorption of electro-magnetic energy by a material results in a reversible change of its color. The activating radiation is in the near ultraviolet or blue part of the visible spectrum. The photochromic material is usually more intensely colored in the activated state than in the initial state. In many cases the reverse reaction involves crossing a potential energy barrier, the energy being supplied either thermally or by optical excitation. The important characteristics of a photochromic system include absorption spectra and extinction coefficients of the parent compound and of the photoproduct, as well as the effect of environmental factors such as solvent and temperature. Photochromic molecules have served for a variety of information recording applications. Examples are chemical switches for computers, signal processors, reusable information storage media, micro-imaging materials, protective materials against irradiations, photomasking and photoresisting materials, to mention a few.

There were two aspects for the motivation to trap organic photochromic dyes: First, the currently used photochromic glasses are based on a very limited selection of inorganic dopants. On the other hand, the ability to trap these dyes in sol-gel glasses [112,113] opens the possibility to use the thousands of organic photochromic molecules with the ability to tailor desired properties such as the nature of color change, the activating wavelength, the rates of response to light and of the subsequent fading, etc. The feasibility of this idea was first demonstrated briefly in reference 114 in which the trapping of the photochromic dye Aberchrome-670 in SiO_2 was described. Difficulties with long-lasting activity of that dye, have shifted the attention to the largest class of photochromic molecules, namely to the spiropyranes. The second aspect is to use the sensitivity of the photochromic process to environmental parameters in order to follow the structural and chemical changes that occur along the formation of the trapping gel-glass, especially along the gel-xerogel transition [112,113].

Fig. 10 presents the photochromic response for a number of spiropyrane dyes trapped in silica-gel glass (SiO_2 glasses). Spectral changes, substituent effects describable in terms of the Hammett equation, and photochromic kinetic changes were studied, in analyzing the response of the photochromic reaction to a continuously changing environment [112]. A common observation for all the photochromic compounds used has been that photochromism (pm) changes gradually to reversed-photochromism (rpm) along the gel-xerogel transition. (The stable forms of the spiropyrane dyes in the dark are the colored ones, which could be bleached then by UV irradiation) (Fig. 11). Photochromic compounds were also used for the investigation of the sol-gel-xerogel transition of $Si(OCH_3)_4$ [112].

The changes from pm to rpm could be rationalized in terms of both the accompanying changes in the environmental polarity and a gradual change in the environment of the photochromic molecule [112]. This molecule passes from a liquid solution medium to an

adsorption on the surface of the gradually forming SiO_2. Molecular isomerizations as a result of irradiation become restricted as the polymerization proceeds, because of the reduction in the size of the effective "free-volume" for these rotations: The photochromic materials are stabilized by strong hydrogen bonds to the silanols of the silica cage in the SiO_2 glasses. These photochromic materials suffered from two problems: The photochromism was reversed and, even more limiting, the photochromism stopped at the final dry xerogel stage. The final material obviously could not have any practical applications.

We solved these problems by applying pore surface variations of the cage of the SiO_2 entrapped molecules [113]. Thus, we have prepared silane-ethyl glasses (SE glasses) by polymerising the CH_3CH_2-$Si(OC_2H_5)_3$ forming an apolar cage surface composed of Si-CH_2CH_3 groups which do not stabilize the colored form of the trapped dye; hence, normal phtochromism is obtained. On the other hand, co-polymerization of $Si(OCH_3)_4$ with polydimethylsiloxanes (pdms, SP glasses) induces sufficient flexibility into the matrix, allowing reversed photochromism in the final glass. The reversed photochromism in the SP glasses might be understood in similar terms to those of the SiO_2 glasses, i.e., in the final glass, the immediate environment is of Si-OH groups, and not of the added pdms. In the SE glasses (Fig. 11), this necessary flexibility is obtained from the reduced cross-linking in the final xerogel: only three of the Si bonds participate in the polymerization, compared to four in the pure SiO_2 glasses. Therefore, the direction of photochromism, either normal (pm) or reversed (rpm), is controllable; and the photochromism properties are retained in the final material with good stability. Reversed photochromism of spiropyranes was observed in sol-gel glass obtained from the polymerization of $Si(OCH_3)_4$ [112] and also, as reported by Matsui et al. [115] from $Si(OCH_2CH_3)_4$. In these unmodified glasses, the photodynamics slow down significantly in the aged glass, due to the high rigidity of the final cage. However, the two organically modified glasses described above provide long lasting active

materials. The added flexibility of those matrices is the direct cause of that improvement.

Stable photochromic materials were also obtained by encapsulating a number of spiropyranes in alumino-silicate sol-gel glasses [83]. These were obtained by the polymerization of $(CH_3CH_2CH_2CH_2O)_2AL\text{-}O\text{-}Si(OCH_2CH_3)_3$. The photochromic properties of these materials were used for the investigation of this polymerization.

5.4. Various other doped Sol-gel materials for optical applications (Addendum).

Several studies were carried out on non-linear optical (NLO) properties of organic molecules in sol-gel matrices [97-104]. Prasad et al. have successfully synthesized silica gel/conjugated polymer composites containing up to 50% (by weight) polymer [103]. These materials have a non-linear response in the subpicosecond range. Prasad also reported the fabrication of two-dimensional gratings using the silica conjugated polymer films and demonstrated the feasibility of using these films for optical recording [103]. Toussaere et al. [100] prepared thin films free from ionic species (1-100 μm) containing non-linear optically active organic molecules via the chemical design of alkoxide precursors and by a careful control of the polymerization mechanism. Recent work of Nakamura et al. [101] showed third order non-linear susceptibility, $\chi^{(3)}$ for 4'-dimethylamino-N-methyl-4-stilbazolium iodide [DMSI] of $4\text{-}5x10^{-14}$esu, twice as large as that of SiO_2 glass.

Another sol-gel approach was used in the preparation of thin-film glasses embodying laser dyes by a fast sol-gel method at elevated temperatures (25-70°C) [102]. Incorporation of a dye-embodying silica precursor gel layer into a three-layered assembly resulting in a supported crack-free glass thin-film of thickness up to 80 μm. These SiO_2 glass films provide a promising route for nonlinear optics applications such as a two-dimensional dye laser system.

Dire et al. [116] reported new preparation techniques of sols of various metal alkoxides. Due to the rheological properties of the sols and the presence of siloxane chains and hydrophobic methyl groups an easy film deposition on glass sheets can be obtained. Rhodamine 6G and Coumarin 4 were incorporated in these films reaching high dye concentrations ($>10^{-2}$M).

Canva et al. [117,118] reported another interesting application for the preparation of an optical gel memory in which by application of a strong polarized electric field on encaged rhodamine 640 alignment of these molecules can be achieved, thus determining a local birefringence. This change in the optical properties of the material is permanent for several days and such optical information can often be deleted or rewritten.

Acknowledgments: We are deeply indebted to our co-workers who made all this progress possible: S. Druckman, I. Gigozin, B. Iosefzon-Kuyavskaya, V.R. Kaufman, I. Kuselman, Dan Levy, J.M. Oton, J.M.S. Pena, S. Rappoport, R. Reisfeld, C. Rottman, C.J. Serna, A. Serrano, S. Shtelzer, A. Slama-Schwock, M. Tsionski, I. Zamir, R. Zusman. We gratefully acknowledge support for various parts of this comprehensive project by the following granting foundations: MT 90/0791 of the CICYT (Spain), The US Army Research, Development and Standardization Group (UK), The Krupp Foundation, the Israel National Council for Research and Development, KFK-Karlsruhe (BMFT) and the Kaye Foundation. D.A. is a member of the F. Haber Research Center for molecular Dynamics and of the Farkas (Minerva) Center for Light Energy Conversion.

REFERENCES

[1] Scherer, G. and Brinker, J. (1990) *Sol-Gel Science,* Academic Press: San-Diego.

[2] *Sol-Gel Technology,* Klein, L.C. Ed., (1990). Noyes Publications, USA.

[3]. Avnir, D., Reisfeld R. and Levy, D., (1983) Israel Patent Application 69724, Sept. 23.

[4] Levy, D., (1984) M.Sc. Thesis, The Hebrew University, Jerusalem.

[5] Avnir, D., Levy, D. and Reisfeld, R. (1984), *J. Phys. Chem.*, **88**, 5956.

[6] For a review, see: (a) Avnir, D., Braun, S. and Ottolenghi, M., *Supramolecular Architecture in Two and Three Dimensions*, (1991), T. Bein, ed., *ACS Symposium Ser.* No. 499, Chapter 27.

(b) Levy, D., (1992), *J. Non-Cryst. Solids* in press.

[7] Bein, T., Brown, K., Frye, G.C. and Brinker, C.J., (1989), *J. Amer. Chem. Soc.*, **111**, 7640.

[8] Grattan, K.T.V., Badini, G.E., Palmer, A.W. and Tseung, A.C.C., (1991), *Sensors and Actuators A* **25-27**, 483.

[9] Philipp, G. and Schmidt, H. (1984), *J. Non-Crystal. Solids*, **63**, 283.

[10] Unger, K.K., Porous Silica (1979), Elsevier Scientific Pub. Company, Amsterdam.

[11] Tsionsky, M., et al. (1992), in preparation.

[12] Ache, H.J. (1992), private communication.

[13] Ref. 1, p. 850-851.

[14] Hench, L.L., (1986), in *Science of Ceramic Chemical Processing*, Hench, L.L. and Ulrich, D.R. Eds., Wiley, New York, p. 52-64.

[15] Iosefzon-Kuyavskaya, B., Gigozin, I., Ottolenghi, M., Avnir, D. and Lev, O., (1992), *J. Non-Cryst. Solids*, in press.

[16] Levy, D., Iosefzon-Kuyavskaya, B., Gigozin, I., Zamir, I., Avnir, D., Ottolenghi, M. and Lev, O., (1992), *J. of Separation Science and Tech.* **27**, 589.

[17] Rottman, C., Ottolenghi, M., Zusman, R., Lev, O., Smith, M., Gong, G., Kagan, M.L. and Avnir D., (1992), *Mater. Letters*, **13**, in press.

[18] Seitz, W.R., (1988), *CRC Crit. Rev. Anal. Chem.*, **19**, 135.

[19] Wolfbeis, O.S., (1990), *J. Anal. Chem.*, **337**, 522.

[20] Majors, R.E., (1977), *J. of Chromatographic Science* **15**, 334.

[21] Stahl, E. (1969), *Thin Layer Chromatography, A Laboratory Handbook*, 2nd Ed., Springer-Verlag, Berlin

[22] Myasoedova, G.V. and Savin, S.B., (1986), *CRC Crit. Rev. Anal. Chem.* **17**, p. 1.

[23] Murray, R.W., (1983) in *Electroanalytical Chemistry*, Bard, A.J. Ed., Marcel Dekker, Inc., NY, **13**, p. 191.

[24] Norris, J.O. (1989) *Analyst* **114**, 1359.

[25] Rakhman'ko, E.M., Yegorov, V.V., Gulevich, A.L. and Lushchik, Ya. F. (1991) *Selective Electrode Rev.*, **13**, 5.

[26] Moody, G.J. and Thomas, J.D.R. (1991) *Selective Electrode Rev.* **13**, 113.

[27] Lev, O., Iosefzon-Kuyavskaya, B., Tsionsky, M., Avnir, D. and Ottolenghi, M., (1992) SPIE Proceedings, Vol. 1716, in preparation.

[28] Zaytsev, V.N. and Trophymchuk, A.K. (1984) *Ukraine Chem. J.* **50**, 1126.

[29] Kuselman, I., et al., (1992), in preparation.

[30] Ikoma, S., Kawakita, K. and Yokoi, H., (1990) *J. Non-Cryst. Solids* **122**, 183.

[31] Zusman, R., Rottman, C., Ottolenghi, M. and Avnir, D., (1990) *J. Non-Cryst. Solids*, **122**, 107.

[32] Nogami, M., Nagaska, K. and Kato, E. (1990) *J. Am. Ceram. Soc.* **73**, 2097.

[33] Zink, J.I. and Dunn, B., (1991) *Japan J. Ceram. Soc.*, in press.

[34] Frye, G.C., Brinker, C.J., Ricco, A.J., Martin, S.J., Hilliard, J. and Doughty, D.H. (1990) *Mat. Res. Soc. Symp. Proc.* **180**, 583.

[35] Knobbe, E.T., Dunn, B. and Gold, M., (1988) *SPIE Proceedings* **906**, 39.

[36] Chernyak, V., Reisfeld, R., Gvishi, R. and Venezky, D., (1990) *Sensors and Materials* **2**, 117.

[37] Eyal, M., Gvishi, R. and Reisfeld, R., (1987) *Journal De Physique* **C7**, 471.

[38] Braun, S., Rappoport, S., Zusman, R., Avnir, D. and Ottolenghi, M. (1990) *Mat. Lett.* **10**, 1.

[39] Rottman, C., Ottolenghi, M., Zusman, R., Lev, O., Smith, M., Gong, G., Kagan, M.L. and Avnir D., (1992) *Mater. Letters* **13**, in press.

[40] Badini, C.E., Grattan, K.T.V., Palmer, A.W. and Tseung, A.C.C., (1989) *Springer Proceedings in Physics* **44**, 36, Ardity, H.J., Dakin, J.P. and Kersten, R.Th., Eds., Springer-Verlag, Berlin.

[41] MacCraith, B.D., Ruddy, V., Potter, C., O'Kelly, B. and McGilp, J.F., (1991) *Electron Lett.* **27**, 1247.

[42] Ding, J.Y., Shahriari, M.R., Sigel, Jun. G.H., (1991) *Electron Lett.*, **27**, 1560.

[43] Dulebohn, J.I., Van Vlierberge, B., Berglund, K.A., Lassard, R.B., Yu, J.-A and Nocera, D.G. (1990) *Mat. Res. Soc. Symp. Proc.* **180**, 733.

[44] Lev, O., Iosefzon-Kyavskaya, B., Gigozin, I., Ottolenghi, M. and Avnir, D., (1992) *Fresenius J. Anal. Chem.*, in press.

[45] Kusnetz, H.L., Saltzman, B.E., and Lanier, M.E., (1960) *Amer. Ind. Hyg. Assoc. J.*, **21**, 361.

[46] Avnir, D., Ottolenghi, M., Braun, S., Zusman, R. and Lev, O. (1990), world-wide patent application pending.

[47] Kuselman, I., Iosefzon-Kuyavskaya, B. and Lev, O. (1992) *Analytica Chimica Acta* **256**, 65.

[48] Kuselman, I., et al. submitted, Talanta, 1992.

[49] Shulz, J.S., Mansuri, S., and Goldstein, I.J. (1982) *Diabetes Care* **5**, 245.

[50] Braun, S., Rappoport, S., Zusman, R., Shtelzer, S., Druckman, Sh. Avnir, D., and Ottolenghi, M. (1991) in *Biotechnology: Bridging Research and Applications*, Makely, D., Chakrabarty, A., and Kornguth, S.E. Eds., pp. 205-218, Kluwer Acad. Publ., Boston.

[51] Ottolenghi, M., Lev, O., Braun, S. and Avnir, D., (1992) *SPIE Proc. Ser. 1758, Sol-Gel Optics II*, Mackennzey, J.D., Ed., San Diego, in press.

[52] S. Shtelzer, S. Rappoport, D. Avnir, M. Ottolenghi and Braun, S. (1992) *Biotechnol. Appl. Biochem.*, in press.

[53] Braun, S., Shtelzer, S., Rappaport, S., Avnir, D., and Ottolenghi, M. (1992) *J. Non-Cryst. Solids*, in press.

[54] Norde, W., and Lykelema J. (1979) *J. Colloid Interface Sci.* **71** , 350.

[55] Lykelema, J. (1984) *J. Colloid Surf.* **10**, 33.
[56] Hench, L.L., and Wilson, J. (1990) *Mat. Res. Soc. Symp. Proc.* **180**, 1061.
[57] Ngo, T.T., and Lenhoff, H.M. (1980) *Anal. Biochem.* **105**, 389.
[58] Ellerby, L.M., Nishida, C.R., Nishida, F., Yamanaka, S.A., Dunn, B., Valentine, J.S., and Zink, J.I. (1992) *Science* **225**, 1113.
[59] Levy, D., Serna, C.J. and Oton, J.M. (1991) *Mat. Lett.*, **10** 470.
[60] Levy, D., Oton, J.M. and Serna, C.J. (1991) Spanish Patent Application 91013
[61] Oton, J.M., Serrano, A., Serna, C.J. and Levy, D. (1991) *Liq. Cryst.*, **10**, 733.
[62] Bellare, J.R., Davis, H.T., Miller, W.G. and Scriven, L.E., (1990) *J. Colloid. Interf. Sci.*, **136**, 305.
[63] Levy, D., Pena, J.M.S., Serna, C.J. and Oton, J.M., (1992) *J. Non-Cryst. Solids*, in press.
[64] Levy, D., Serna, C.J., Serrano, A. and Oton, J.M. (1992) *SPIE Proc. Ser. 1758, Sol-Gel Optics II,* Mackenzey, J.(., Ed., San Diego, in press.
[65] Makishima, A. and Tani, T. (1986) *J. Am. Ceram. Soc.* **69**, C-72.
[66] Kobayashi, Y., Imai, Y. and Kurokawa, Y. (1988) *J. Mat. Sci. Lett.* **7**, 1148.
[67] Avnir, D., Kaufman, V.R. and Reisfeld, R. (1985) *J. Non-Cryst. Solids* **74**, 395.
[68] Reisfeld, R., Eyal, M. and Brusilowski, D. (1988) *Chem. Phys. Lett.* **153**, 210.
[69] Pope, E.J.A. and MacKenzie, J.D. (1987) *MRS Bull.*, March 17, 29.
[70] Fujii, T., Ishii, A. and Anpo, M. (1990) *J. Photochem. Photobiol.* **A54**, 231.
[71] Santos, D.I., Aegerter, M.A., Briocurz, C.H., Scarparo, M. and Zarzycki, J. (1986) *J. Non-Cryst. Solids* **82**, 231.
[72] Eyal, M., Reisfeld, R., Chernyak, V., Kaczmarek, L. and Grabowska, A. (1991) *Chem. Phys. Lett.* **176**, 531.

[73] Reisfeld, R., Brusilovski, D., Eyal, M. and Jorgensen, K. (1989) *Chimia* **43**, 385.

[74] Fujii, T., Kawauchi, O., Kurikawa, Y., Ishii, A., Negishi, N. and Anpo, M. (1990) *Chem. Express* **5**, 917.

[75] Reisfeld, R. and Gvishi, R. (1987) *Chem. Phys. Lett.* **138**, 377.

[76] Fujii, T., Ishii, A., Nagai, H., Niwano, M., Negishi, N. and Anpo, M. (1989) *Chem. Express* **4**, 1.

[77] Pouxviel, J.C., Parvaneh, S., Knoble, E.T. and Dunn, B. (1989) *Solid State Ionics* **32/33**, 646.

[78] Matsui, K., Matsuzuka, T. and Fujita, H. (1989) *J. Phys. Chem.* **93**, 4991.

[79] Fujii, T., Mabuchi, T. and Mitsui, I. (1990) *Chem. Phys. Lett.* **68**, 5.

[80] Yamanaka, T., Takahashi, Y. and Uchida, K. (1990) *Chem. Phys. Lett.* **172**, 405.

[81] McKiernan, J., Pouxviel, J.C., Dunn, B. and Zink, J.I. (1989) *J. Phys. Chem.* **93**, 2129.

[82] Winter, R., Hua, D.W., Song, X., Mantulin, W. and Jonas, J. (1990) *J. Phys. Chem.* **94**, 2706.

[83] Preston, D., Pouxviel, J.-C., Novinson, T., Kaska, W.C., Dunn, B. and Zink, J.I. (1990) *J. Phys. Chem.* **94**, 4167.

[84] Gutierez, A.R., Friedrich, J., Haarer, D. and Wolfrum, H. (1982) *IBM J. Res. Div.* **26**, 198.

[85] Locher, R., Renn, A. and Wild, V.P. (1987) *Chem. Phys. Lett.* **138**, 405.

[86] Tanaka, H., Takahashi, J., Tsuchiya, J., Kobayashi, Y. and Kurokawa, Y.K. (1989) *J. Non-Cryst. Solids* **109**, 164.

[87] Tani, T., Namikawa, A., Arai, K. and Makishima, A. (1985) *J. Appl. Phys.* **58**, 3559.

[88] Kobayashi, Y., Kurokawa, Y., Imai, Y. and Muto, S. (1988) *J. Non-Cryst. Solids* **105**, 198.

[89] Sasaki, H., Kobayashi, Y., Muto, S. and Kurokawa, Y. (1990) *J. Am. Ceram. Soc.* **73**, 453.

[90] Dunn, B., Knobbe, E.T., McKiernan, J.M., Pouxviel, J.C. and Zink, J.C. (1988) *Mat. Res. Soc. Symp. Proc.* **121**, 331.

[91] Knobbe, E.T., Dunn, B., Fuqua, P.D. and Nishida, F. (1990) *Appl. Opt.* **29**, 2729.

[92] Salin, F., Le Saux, G., Georges, P., Brun, A., Bagnall, C. and Zarzycki, J. (1989) *Appl. Opt.* **14**, 785.

[93] Dunn, B., this book.

[94] Fitreman, J., Doeuff, S. and Sanchez, C., (1990), *Ann. Chim. Fr.* **15**, 421.

[95] Altman, J.C., Stone, R.E., Dunn, B. and Nishida, F. (1991) *IEEE Photonics Tech. Lett.* **3**, 189.

[96] Canva, M., Georges, P., Brun, A., Larrue, D. and Zarzycki, J. (1992) *J. Non-Cryst. Solids*, in press.

[97] Capozzi, A.C. and Pye, L.D. (1989) *SPIE Proc., Properties and Characteristic Optical Glass*, 970.

[98] Reisfeld, R. (1990) *J.Non-Cryst. Solids*, **121**, 254.

[99] Zink, J.I., Dunn, B., Kaner, R.B., Knobbe, E.T. and McKiernan, J. (1990) *ACS Symp. Materials for Nonlinear Optics*, S.R. Marder Ed., **455** Ch. 36, 541, Boston.

[100] Toussaere, E., Zyss, J., Griesmar, P. and Sanchez, C. (1991) *Nonlinear Optics* **1**, 1.

[101] Nakamura, M., Nasu, H. and Kamiya, K. (1991) *J. Non-Cryst. Solids* **135**, 1.

[102] Haruvy, Y. and Webber, S.E. (1992) *Chem. Mater.* **4**, 89.

[103] Prasad, P.N. (1990) *Mat. Res. Soc. Symp. Proc.* **180**, 741.

[104] Griesmar, P., Sanchez, C., Puccetti, G., Ledoux, I. and Zyss, (1991) *J. Mol. Engineering* **3**, 1.

[105] Reisfeld, R. in *Sol-Gel Science and Technology, (1989)* Aegerter et al., Eds., World Scientific: Singapore (1989), pp. 323-345.

[106] Reisfeld, R. and Seybold, G. (1990) Chimia **44**, 295. Reisfeld, R. et al., (1989) *Chem. Phys. Lett.* **160**, 43.

[107] Nakazumi, H., Amano, S. and Kitao, T. (1991) *Chem. Express* **6**, 607.

[108] Pope, E.J.A., Asami, M. and Mackenzie, J.D. (1989) *J. Mater. Res.* **4**, 1018.

[109] Kaufman, V.R., Levy, D. and Avnir, D. (1986) *J. Non-Cryst. Solids*, **82** 103.

[110] Levy, D. and Avnir, D. (1991) *J. Photochem. Photobiol. A: Chem.*, **57**, 41.

[111] Ueda, M., Kim, H.-B., Ikeda, T. and Ichimura, (1992) K. *Chem. Mater.* in press.

[112] Levy, D. and Avnir, D. (1988) *J. Phys. Chem.*, **92**, 4734.

[113] Levy, D., Einhorn, S. and Avnir, D. (1989) *J. Non-Cryst. Solids* **113**, 137.

[114] Kaufman, V.R., Levy, D. and Avnir, D. (1986) *J. Non-Cryst. Solids* **82**, 103.

[115] (a) Matsui, K., Morohoshi, T. and Yoshida, S. (1988) *Proc. Int. Meet. Adv. Mat., Tokyo.* (b) Morohoshi, T. and Matsui, K. (1989) *Kenkyiu Hokoku* **32**, 229 (*Chem. Abstr.* 1989, 111:47962r).

[116] Dire, S., Babomeau, F., Carturan, G. and Livage, J. (1992) *J. Non-Cryst. Solids*, in press.

[117] Canva, M., Le Saux, G., Georges, P., Braun, A., Chaput, F. and Boilot, J.-P., (1992) *Opt. Letters*, in press.

[118] Canva, M., Le Saux, G., Georges, P., Braun, A., Chaput, F. and Boilot, J.-P., (1992) *J. Non-Cryst. Solids*, in press.

Figure Legends

Figure 1. Glucose Oxidase-Peroxidase Optical Glucose Sensor. Xerogel disk (8 mm in diameter and 2 mm thick) containing glucose oxidase, peroxidase and a chromogenic assay for peroxidase was placed in the optical pathway of the densitometer in a vial containing 3 ml water. At time zero a concentrated solution of glucose was added bringing glucose concentration to 10 mM. Enzymatic oxidation of glucose produced H_2O_2, which in the presence of peroxidase and of the chromogenic assay components resulted in dye formation [53]. Dye accumulation in the sol-gel disk is recorded in arbitrary optical density units. More glucose was added at 6, 8 and 10 min. Glucose concentrations are shown at the arrows.

Figure 2. Glucose Oxidase Reversible Sensor: The spectra of the sol-gel immobilized glucose oxidase at pH 7.0 in the absence (1) and in the presence (2) of 2 mM glucose are shown.

Figure 3. The microdroplets of K15 in a liquid crystal state filling the pores of the sol-gel thin-film at room temperature. The picture is taken with cross-polarizers.

Figure 4. Switching times of phenyl and methyl samples (thickness is 70 μm) for different applied voltages. (LC concentrations are 16 ml and 8 ml per mol of reacting group, respectively). a) Phenyl substrates show nearly constant rise time for the whole range whereas methyl substrates stabilize in the upper region. b) Relaxation times are substantially constant in both substrates, except for the lowest points of the phenyl substrate, below the methyl threshold. c) Normalized contrast ratio. Note the smooth contrast increase in the methyl substrate as compared to the sharp phenyl curve.

Figure 5. Influence of LC concentration on rise time. Methyl substrate, droplet sizes 2-5 μm and 20-50 μm (sample thicknesses are 70 μm). LC concentrations are low: 2 ml, 4 ml and high: 6 ml,

8 ml per mol of reacting group. Note the slow decrease for higher LC concentrations in both droplet sizes.

Figure 6. Absorption spectra of rhodamine 6G: (- - - - - -) 1.4 x 10-4 M in water; the dimer is clearly visible at 496 nm. (——) $1.6x10^{-4}$ M in gel glass. (- - - -) Undoped glass.

Figure 7. Emission spectra of various doped silica or silica-titania sol-gel thin films.

Figure 8. Fluorescence (——) and RTP (----) spectra of 4-BPCA trapped in SiO_2 gel glasses prepared under neutral conditions (A) and when NaBr is present in the starting solution (B). The solution spectra of 4-BPCA (C) was recorded for comparison (10^{-3} M, methanol).

Figure 9. Phosphorescence and/or delayed fluorescence (-----) and fluorescence (——) of 4-BPCA trapped in silica gel-glasses prepared with different [NaOH]: A, 10^{-4} M NaOH; B, 0.5 M NaOH and C, 6M NaOH. $_{ex.}$=290 nm.

Figure 10. Absorption spectra of the SE class of photochromic materials. The colorless base-line before irradiation (b.i.) is also shown.

Figure 11. Changes in the photochromic properties of trapped 5-bromo-8-methoxy-6-nitro-BIPS along the sol-gel-xerogel transition in polymerizing silicon tetramethoxide. ≥: intensity before irradiation; ≥ intensity after irradiation.

Fig 1

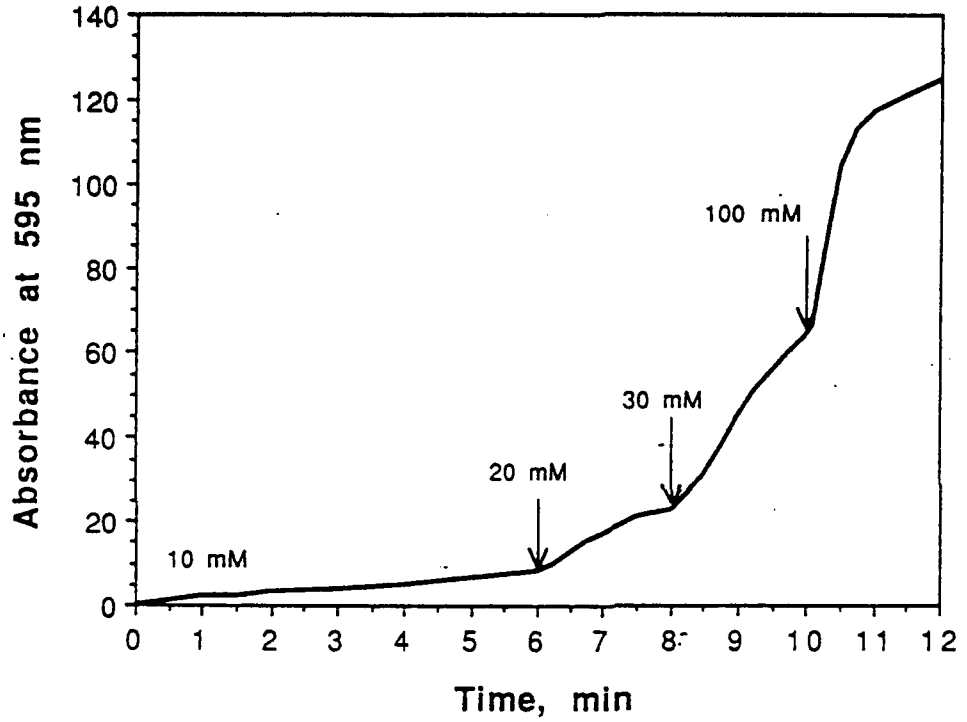
Absorbance at 595 nm
140
120
100
80
60
40
20
0
0 1 2 3 4 5 6 7 8 9 10 11 12
Time, min
10 mM
20 mM
30 mM
100 mM

Fig 2

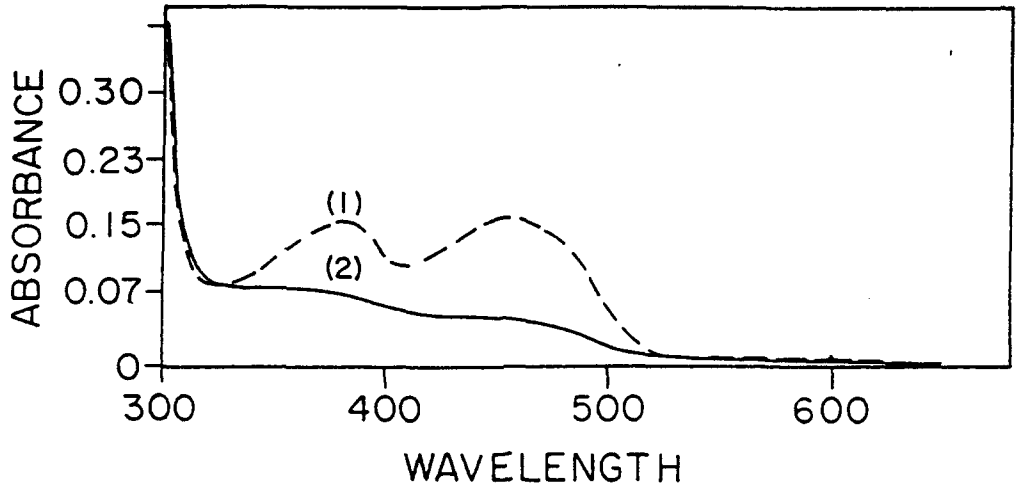

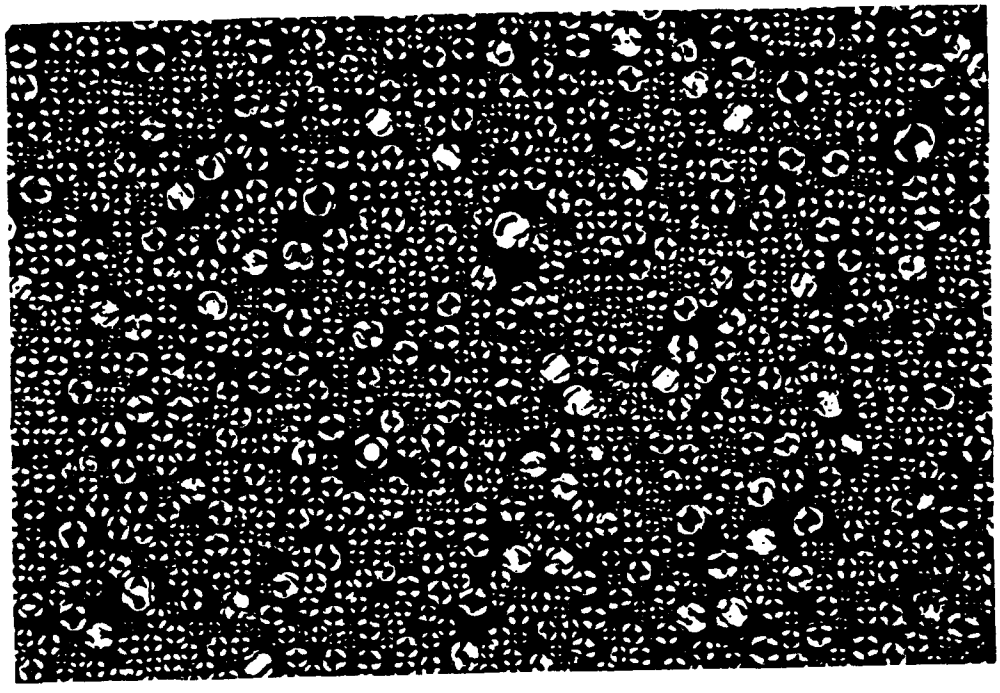

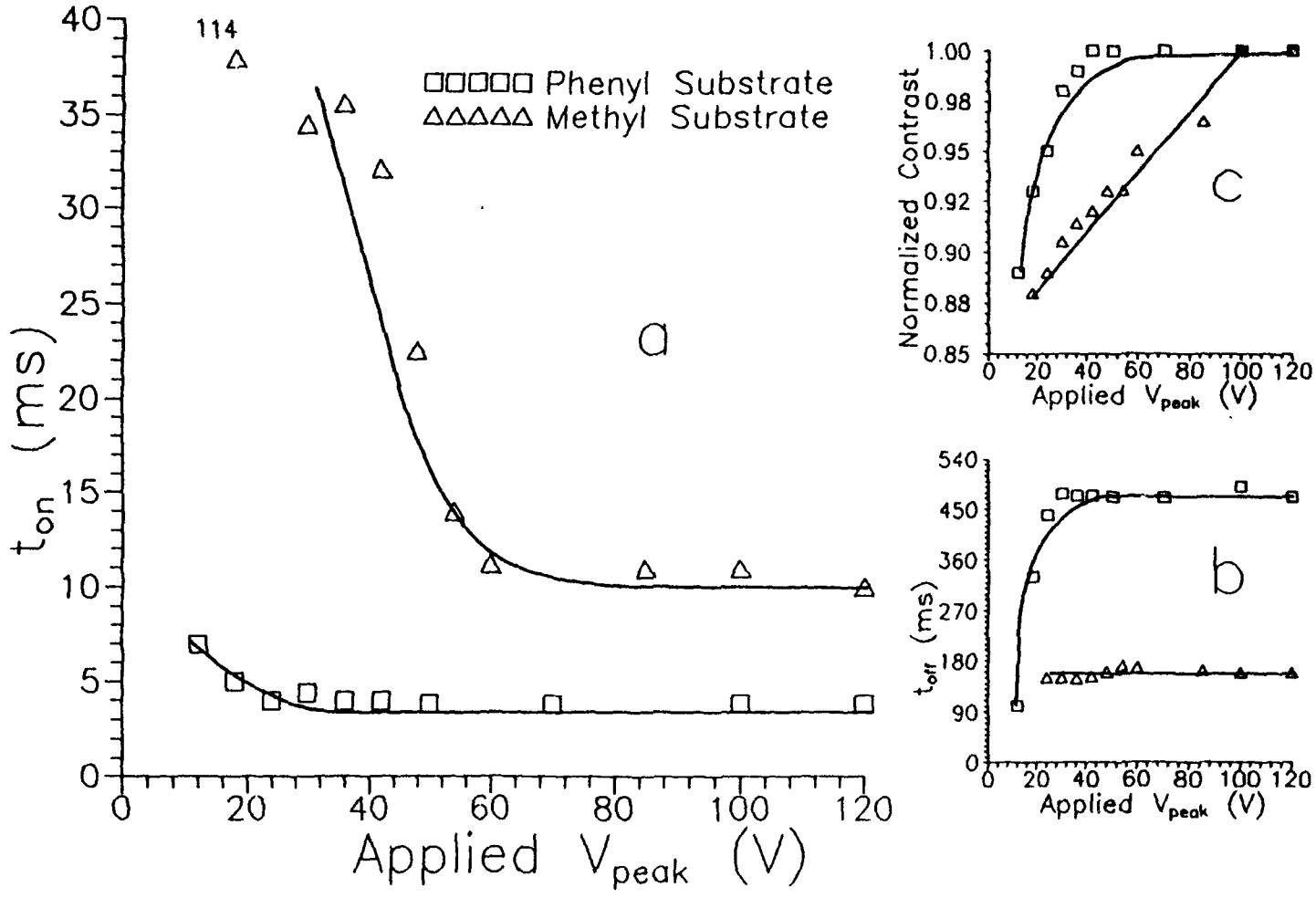
114
□□□□□ Phenyl Substrate
△△△△△ Methyl Substrate
a
t_{on} (ms)
Applied V_{peak} (V)
0
5
10
15
20
25
30
35
40
0
20
40
60
80
100
120

Normalized Contrast
1.00
0.98
0.95
0.92
0.90
0.88
0.85
c
0
20
40
60
80
100
120
Applied V_{peak} (V)

t_{off} (ms)
540
450
360
270
180
90
0
b
0
20
40
60
80
100
120
Applied V_{peak} (V)

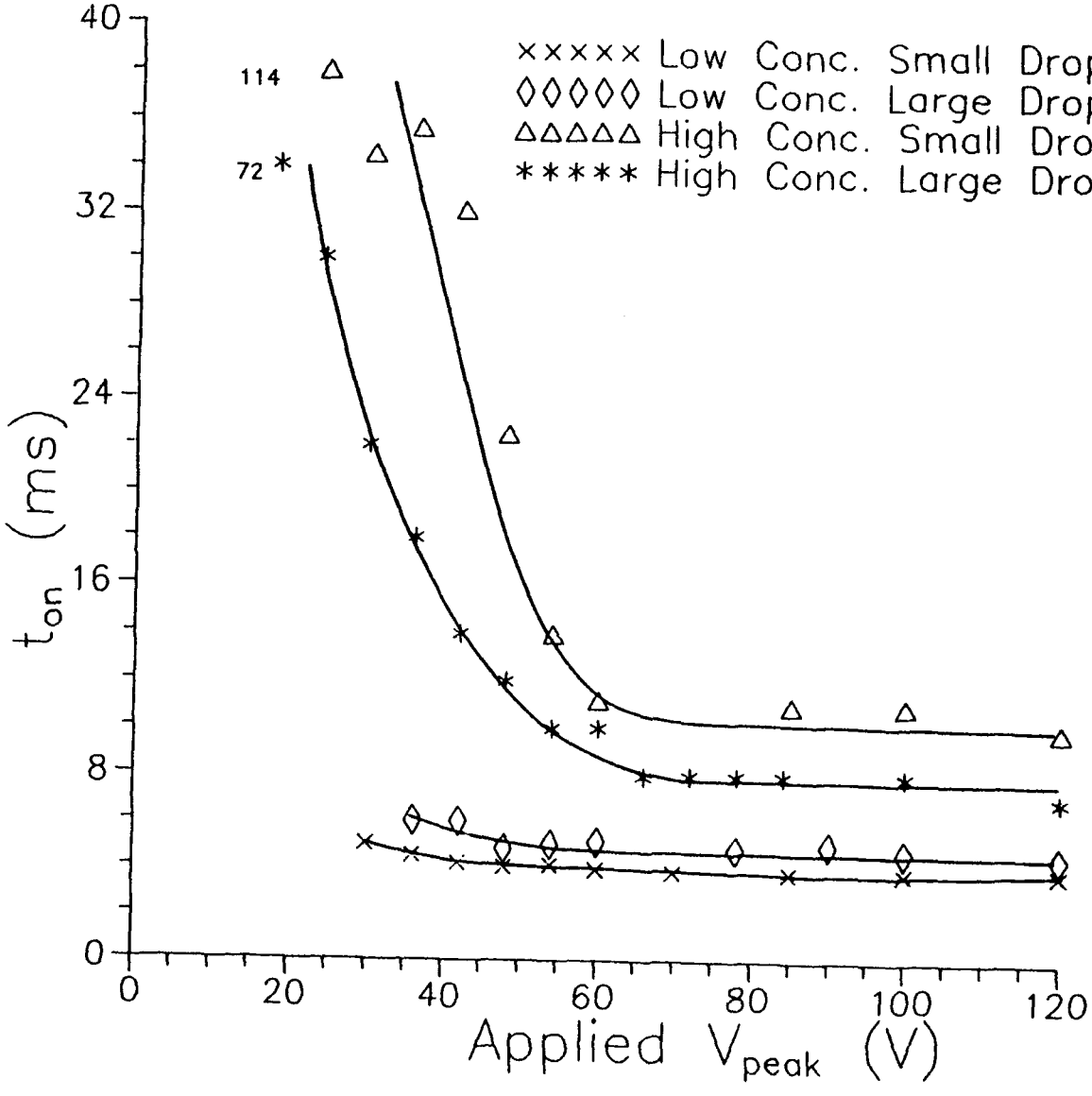
40
32
24
16
8
0
t_{on} (ms)
114
72
××××× Low Conc. Small Droplet
◊◊◊◊◊ Low Conc. Large Droplet
ΔΔΔΔΔ High Conc. Small Droplet
***** High Conc. Large Droplet
0
20
40
60
80
100
120
Applied V_{peak} (V)

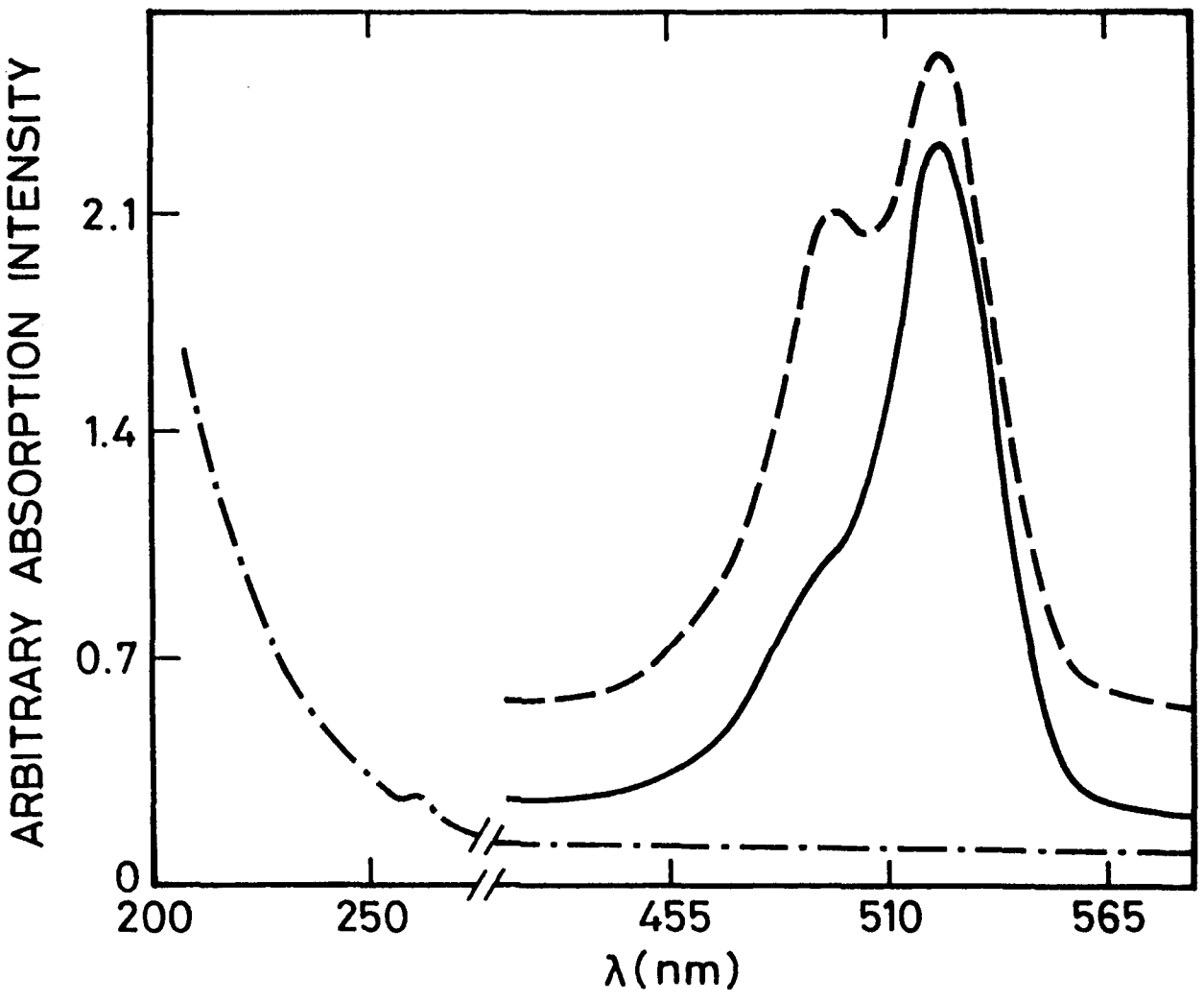
ARBITRARY ABSORPTION INTENSITY
2.1
1.4
0.7
0
200
250
455
510
565
λ(nm)

Fig 7

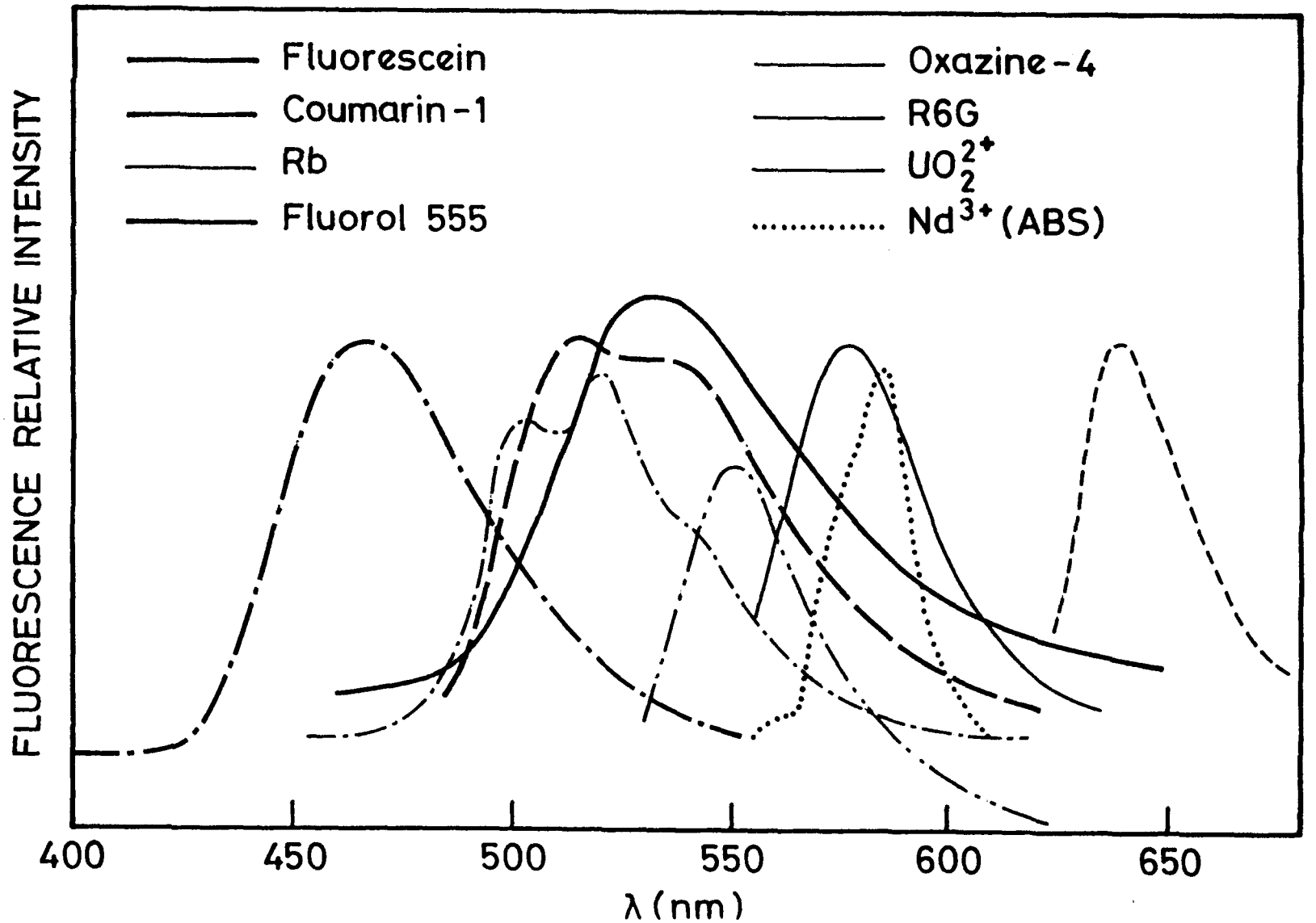
Fluorescein
Coumarin-1
Rb
Fluorol 555
Oxazine-4
R6G
UO_2^{2+}
Nd^{3+} (ABS)
FLUORESCENCE RELATIVE INTENSITY
400
450
500
550
600
650
λ (nm)

Figure 8

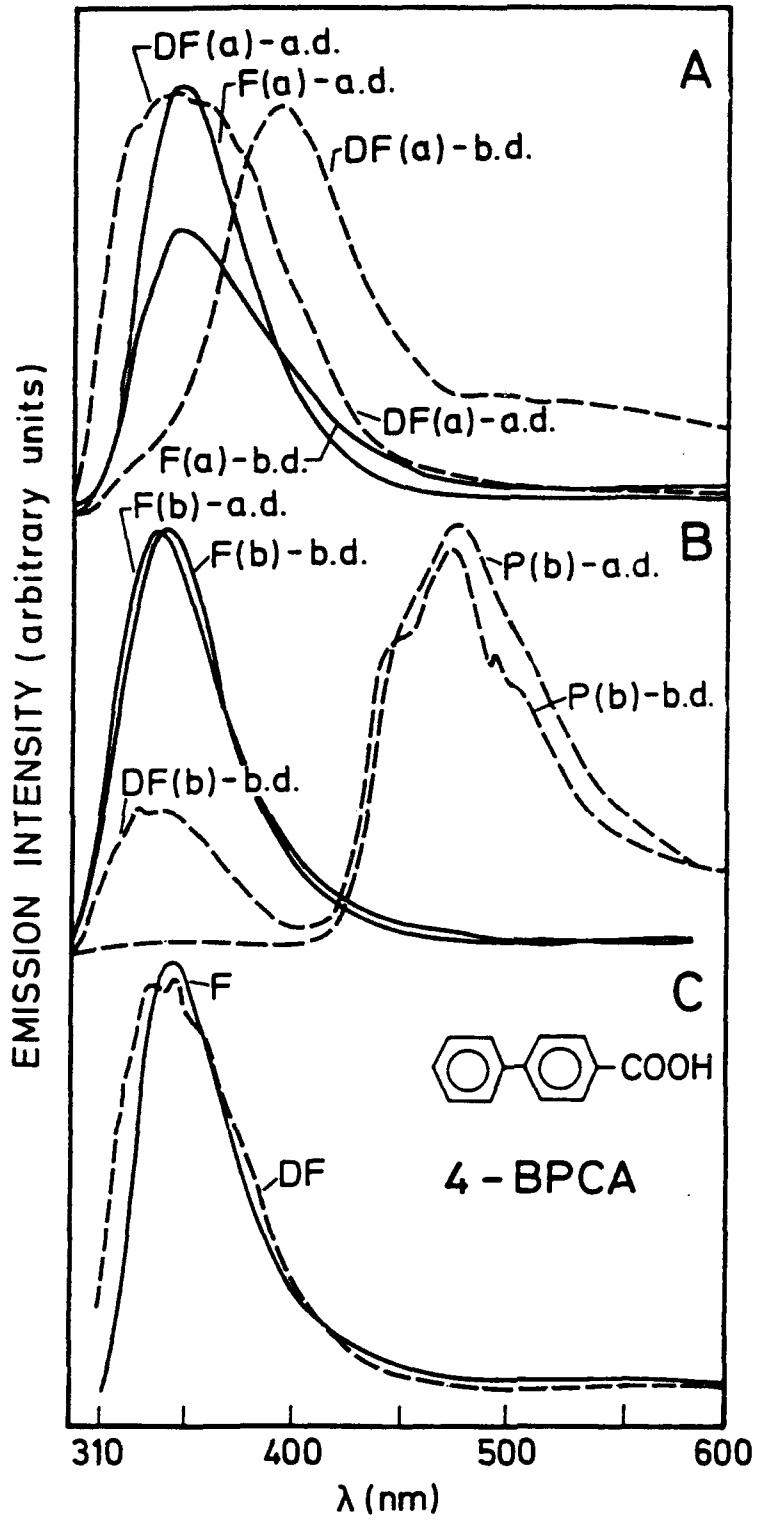
DF(a)-a.d.
F(a)-a.d.
DF(a)-b.d.
A
DF(a)-a.d.
F(a)-b.d.
F(b)-a.d.
F(b)-b.d.
P(b)-a.d.
B
P(b)-b.d.
DF(b)-b.d.
F
C
COOH
DF
4-BPCA
EMISSION INTENSITY (arbitrary units)
310
400
500
600
λ (nm)

Fig 9

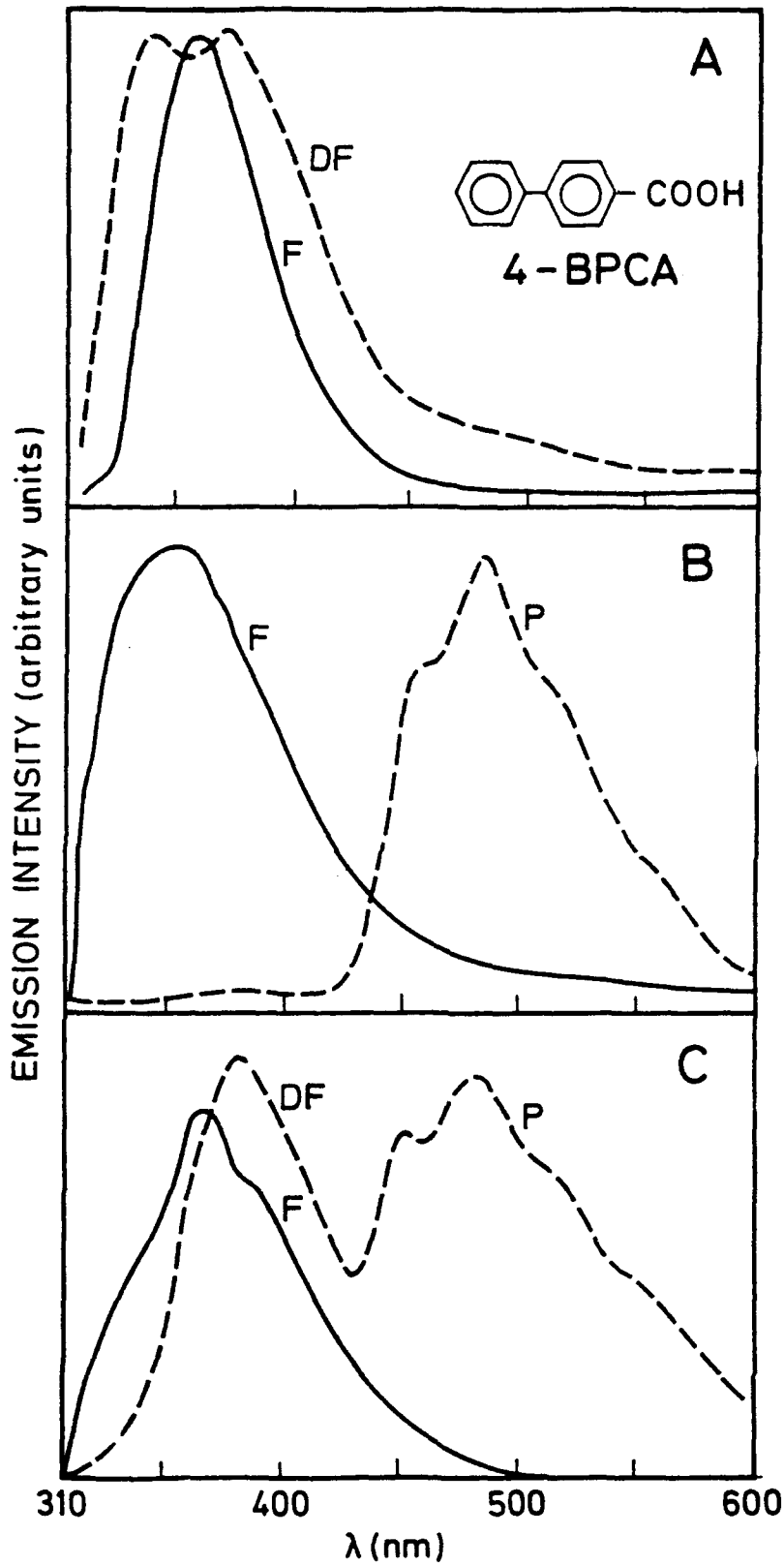
A
DF
F
COOH
4-BPCA
B
F
P
C
DF
F
P
EMISSION INTENSITY (arbitrary units)
310
400
500
600
λ (nm)

Figure 10

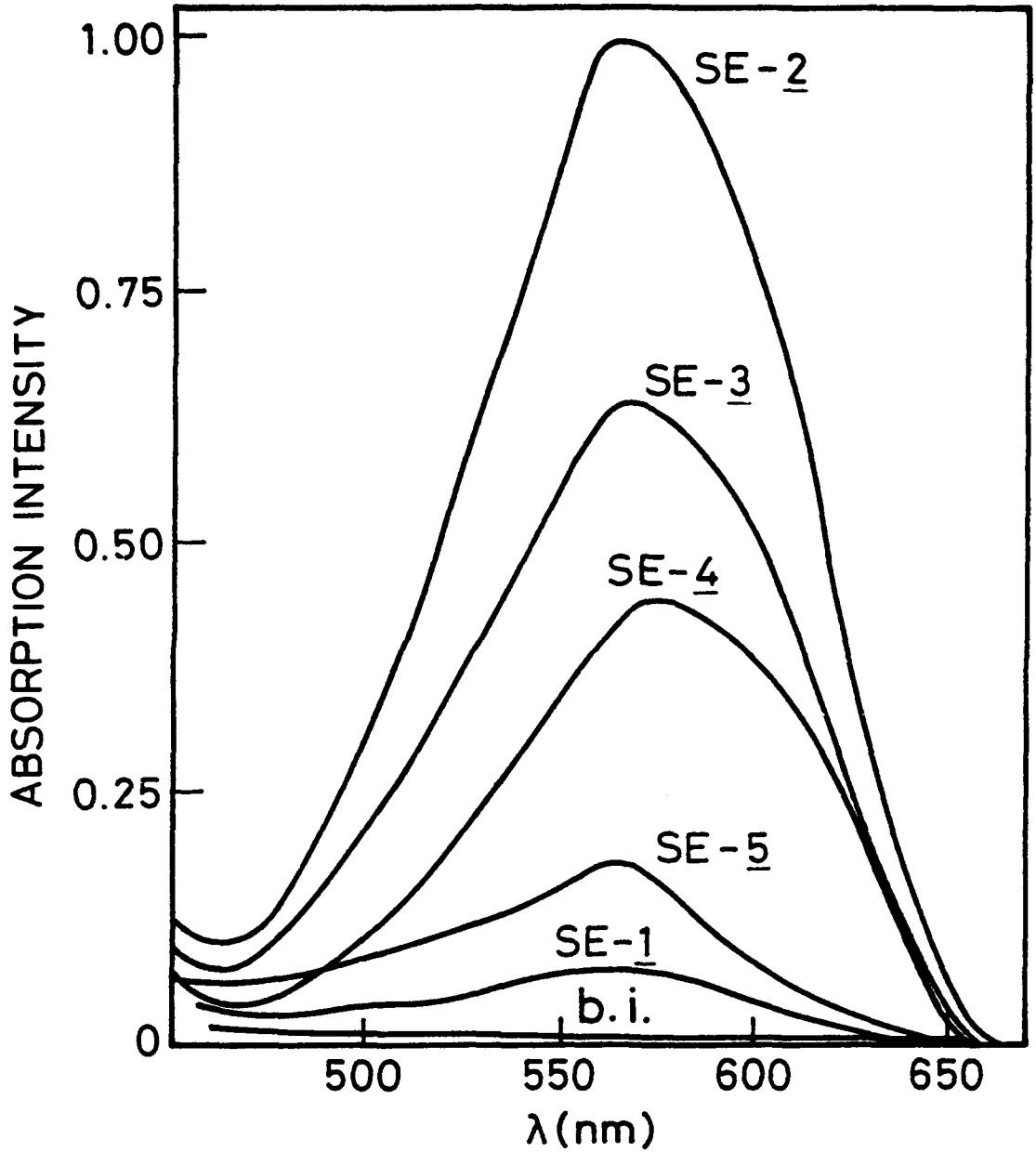
1.00
0.75
0.50
0.25
0
ABSORPTION INTENSITY
SE-2
SE-3
SE-4
SE-5
SE-1
b.i.
500
550
600
650
λ(nm)

Figure 11

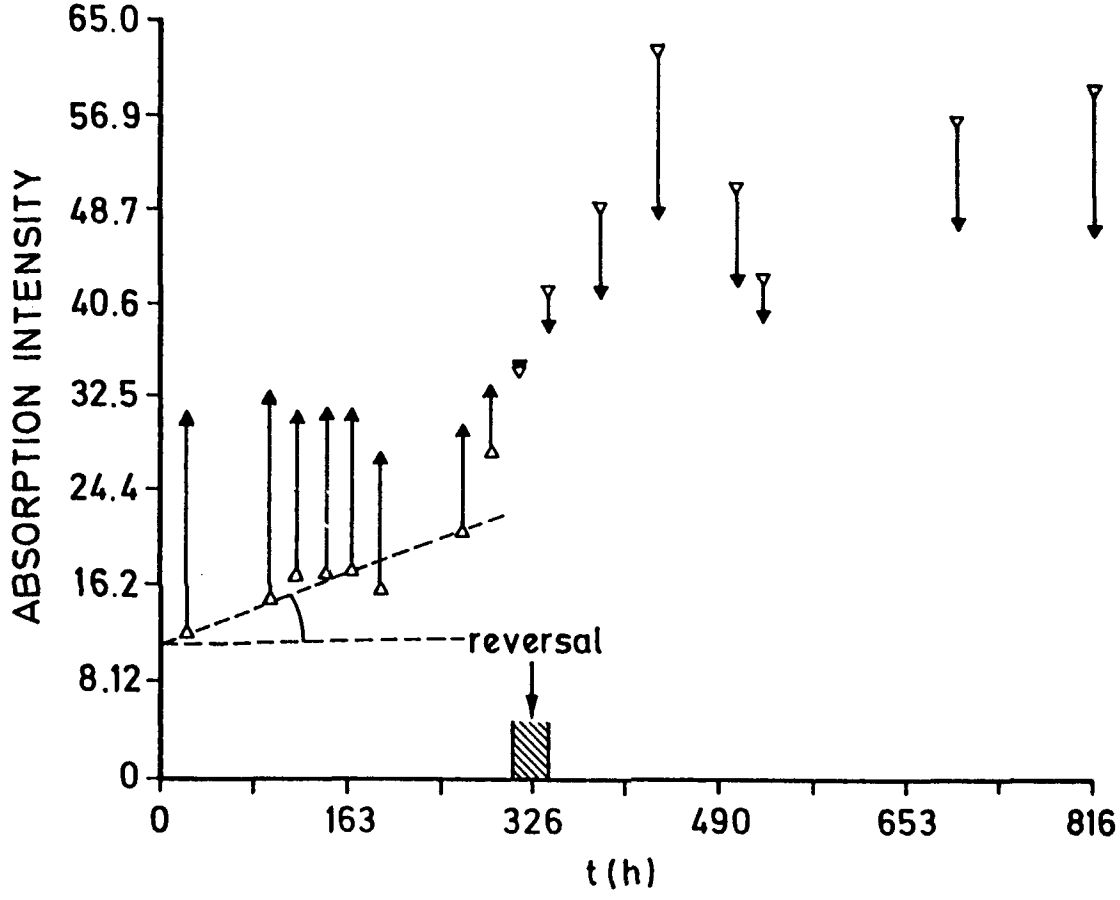
65.0
56.9
48.7
40.6
32.5
24.4
16.2
8.12
0
ABSORPTION INTENSITY
reversal
0
163
326
490
653
816
t (h)